INDIAN BROOK PRELIMINARY FLOOD RISK MODELLING: PHASE II

Prepared by

Tim Webster, PhD
Kate Collins, Nathan Crowell, Kevin McGuigan, Candace MacDonald
Applied Geomatics Research Group
NSCC, Middleton
Tel. 902 825 5475
email: tim.webster@nscc.ca

Submitted to

MI'KMA'KI ALL POINTS SERVICE
P.O. Box 63, Shubenacadie, NS, B0N 2H0

March 28, 2015

Executive Summary

Phase II

In Phase II of the project the continued deployment of the weather station and water level sensor combined with additional flow and stream channel measurements in 2014-2015 allowed for the further refinement and development of the Indian Brook hydrodynamic modelling and results of Phase I. The additional field data were used to calculate a rating curve that sufficiently represented a range of high and low water levels. The rating curve was used to refine and calibrate the 1-D flood risk model and couple it with the 2-D model. The 2-D model was run using a 6 m digital elevation model and was calibrated using high water events from 2013 and 2014 that did not include the effects of melting snow. Once calibrated, the linked 1-D and 2-D model was used to predict the timing and extent of floodwaters under different infrastructure and climate change scenarios.

Precipitation was the main factor considered when evaluating the effect of potential climate change on flood risk of the study area in the future. We used the research of Richards and Daigle (2012) to modify the input precipitation to simulate future flooding events considering climate change. Model results of a 16% increase in rainfall using present infrastructure showed roads were overtopped for a longer duration and experienced deeper floodwaters. This suggests damage to roadbeds and infrastructure would be more severe. It also suggests a higher risk to the safety of community members who may be isolated or put at risk by more frequently flooded roadways.

Additionally in Phase II, the flood risk model was used to test various adaptation measures to mitigate flooding. These included running the model with culverts cleared of sediment buildup, replacing the culverts with bridges, and increasing road heights at the most flood-prone roads. Model results showed that all three scenarios reduced flooding, but that replacing the multi-culvert systems with bridges was the most effective adaptation strategy, by more efficiently routing water to reduce road overtoppings and flood depths.

Phase II also involved the translation of the model output and current GIS database to the Q-GIS open source software and the development of training materials. A GIS workshop was held on February 20, 2015 and was attended by four local officials and three AGRG research associates. The attendees were instructed on the installation and operation of Q-GIS. A geodatabase of Indian Brook spatial data were transferred to the Indian Brook local officials, and they were instructed on how to manage, display and query the data. This will allow the community to better manage and track its infrastructure and assist in land use planning in the future.

Phase III

In Phase III we will work with MAPS to embed the hydrodynamic model into the community's infrastructure maintenance and development planning processes. This will involve using the adaptation simulation results as a basis for the community's interaction with a hydrological engineering firm. We will also work with MAPS to incorporate the flood risk model into the local emergency response protocol; this will involve a quantification of the relationship between rainfall and flooding, so that officials can adequately prepare for potential flooding using a forecasted heavy rainfall event.

The hydrodynamic model will continue to be developed in Phase III, but in a new capacity as a contamination disbursement plan. Drinking water supplies have been contaminated at Indian Brook in the past, necessitating a water management plan. To accomplish this, we will survey subsurface infrastructure in the Indian Brook Watershed, examine and map sources of fecal coliform, and develop a contamination disbursement model to be linked with the Mike 1-D/2-D hydrodynamic model. The model will be used to develop a water management plan for the community and reduce contamination of drinking water sources.

The completion of the incorporation of traditional knowledge, model results and spatial data including lidar and orthophoto products into a geodatabase will occur in Phase III, and we will present and summarize all the deliverables from Phases I, II and III at a final community meeting.

Table of Contents

Table of Figures

List of Tables

1 Introduction

Indian Brook First Nation is the second largest Mi'kmaw community in Nova Scotia, inhabiting 1195 members on 1,234 hectares. Brooks and wetlands encompass about one third of the land base. Fluvial flooding is a problem for Indian Brook First Nation with the current intensity and duration of precipitation events, and increased residential development has caused the community to expand into flood-prone areas. Intense or prolonged rain events, melting snow and ice, or a combination of the two cause property and infrastructure damage more frequently than in the past.

The objective of this study is to develop a GIS-based hydrodynamic model of flood extent in the community of Indian Brook during present day conditions, and under climate change scenarios expected in the future. In Phase I, a preliminary hydrodynamic model was developed that generated flood inundation maps of the community. In Phase II, the model was calibrated and refined, and used to simulate various climate change scenarios. Terrain, culverts and infrastructure were modified to simulate various adaptation measures; the results provided to Indian Brook will allow them to move forward with obtaining costs estimates from an engineering firm for implementation of their chosen adaptation measures.

In order for this initiative to come to fruition and reach its potential benefits in both existing and planned developments on Indian Brook, there was a need to establish and transfer a baseline GIS capacity to Indian Brook. This was accomplished as part of the Phase II deliverables at a GIS workshop on February 20, 2015. The transfer of GIS data as a modelling tool kit will allow local officials and community members the opportunity to use the model to generate various informed scenarios related to climate change, facilitating approaches for adaptive or remedial responses. Additionally, the modelling tool will be integrated into community planning strategies in the form of best practices, new development planning considering climate change, and effective emergency response guidelines.

The flood risk analysis of the Indian Brook First Nation completed here for Phase II utilizes high-resolution lidar elevation data to derive a digital elevation model (DEM). Similar methodology has been followed in previous studies as part of the Atlantic Climate Change Adaptation Solutions (ACAS) project (Webster et al., 2011, 2012a, 2012b, 2012c). We employ the Danish Hydraulic Institute (DHI) coupled 1-D/2-D Mike Flood™ model which integrates a one-dimensional numerical model of the river channel with a two-dimensional model of the floodplain. This model is a common choice for flood prediction mapping using lidar-based DEMs (Gilles et al., 2012; Patro et al., 2009). Gilles et al. (2012) modeled fluvial flood events in Iowa successfully by calibrating the model to measured water levels in the river and floodplain. Patro et al. (2009) modeled monsoon flooding on an Indian river delta and found the model to be quite satisfactory in simulating river flow and flood inundation extent.

1.1 GIS Workshop

A GIS workshop was held on February 20, 2015 and was attended by four local officials and three AGRG research associates. The attendees were instructed on the installation and operation of QGIS, an open source (free) GIS platform. A geodatabase of Indian Brook spatial data were transferred to the Indian Brook local officials, and they were instructed on how to manage, display and query the data.

1.2 Recent flooding

Several high water events and resulting flooding have occurred in the Indian Brook community since the beginning of this study. November 28, 2013 saw 57.4 mm of rain and caused a road washout (Figure 1.2), and between Dec. 3 and 4 approximately ~77 mm of rain fell, causing roads to flood and ditches to overflow (Figure 1.3). Through the winter and spring there were several other high water events (Figure 1.4) that involved snow and ice, but the summer that followed was very dry. November and December of 2014 saw high precipitation events and much flooding. ~60 mm of rain fell on November 17 and 18 (Figure 1.5a), followed by another ~60 mm on November 26 and 27 (Figure 1.5b-d). Between December 11 and 12 105.6 mm of rain fell at Indian Brook causing wide scale flooding and road washouts (Figure 1.6).

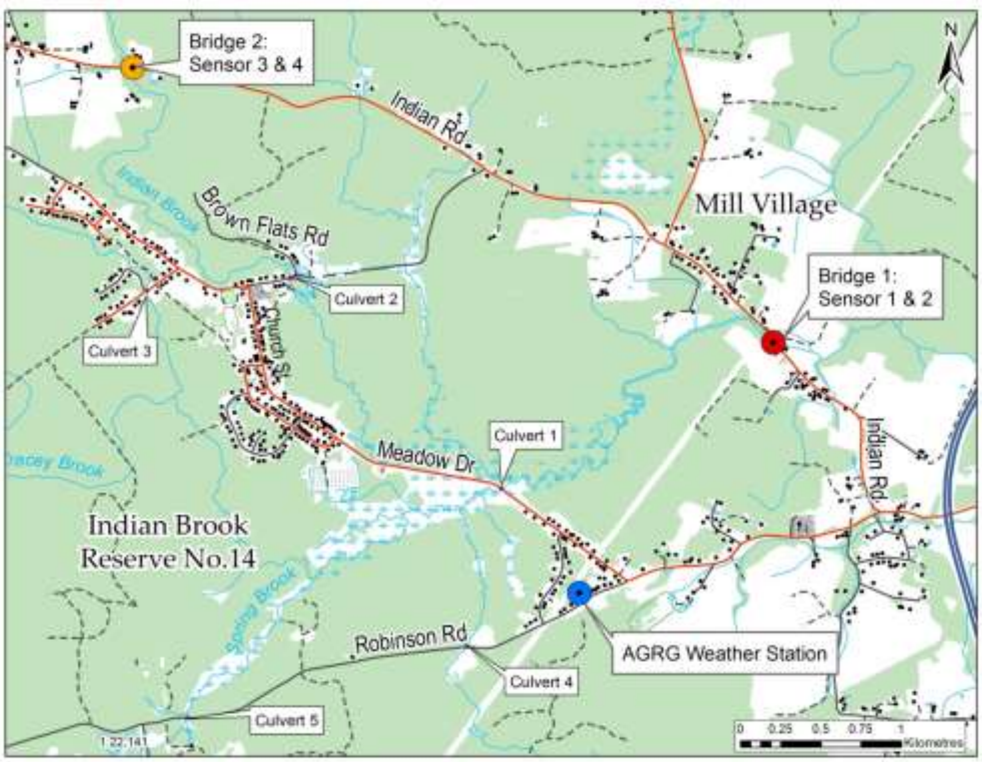

Figure 1.1: Map of the reserve showing street names to use when referring to flood photos. Note location of Indian Road, Brown Flats Road, and Meadow Drive.

Figure 1.2: Flooding on November 28, 2013. (a,b) Culvert 1 at Meadow Drive; (c,d) Culvert 2 and washout at Brown Flats Rd. Photo source: MI'KMA'KI All Points Services.

Figure 1.3: December 4, 2013 flooding. (a,b) Washed out road at Brown Flats Road near apartments near Culvert 2; (c) Meadow Drive near Culvert 1; (d) Robinson Road (e) Culvert 2 near Brown Flats Road (f) Meadow Drive near Culvert 1. Photo source: MI'KMA'KI All Points Services.

Figure 1.4 (a,b) March 13, 2014 at Robinson Road; (c,d) March 31, 2014 at Meadow Drive.

Figure 1.5 (a) November 18, 2014 at Brown Flats Road; (b-d) November 27, 2014 at Meadow Drive, Robinson Road, and Brown Flats Road, respectively.

Figure 1.6: Flooding on December 11, 2014. (a, b) at Meadow Rd, (c,d) at Brown Flats Road.

1.3 Climate change scenarios

As is the case with temperature and sea-level, precipitation and river discharge patterns are changing with climate change. In studies of precipitation in Atlantic Canada during the last half of the 20th century, Bruce et al. (2000) report an increasing trend in the number of daily precipitation events > 20 mm, and Mekis and Hogg (1999) note an increase in the fraction of total precipitation falling in heavy events.

There are many different scenarios for how precipitation patterns will continue to change with climate change, although there does seem to be consensus that there will be much more variability in the amount and frequency of intense rainfall in Nova Scotia (Bruce et al., 2000; Natural Resources Canada, 2010; Richards and Daigle, 2011) and in the Northeastern United States (Madsen and Willcox, 2012; Singh et al., 2013; Toreti et al., 2013). Richards and Daigle (2011) project a variety of climate variables into the future based on an ensemble of several climate models. For Truro, the nearest station to Indian Brook, they predict an annual increase in precipitation; most of that increase is predicted to occur in the winter and spring, with minimal increase in summer and fall precipitation (Table 1). Extreme rainfalls that happened only once every 50 years in the last century could occur once every 10 years in this century (NS Dept. Env., 2009), and precipitation is expected to vary more from season to season and from year to year. Natural Resources Canada (NRCan) (Natural Resources Canada, 2010) predicts that Atlantic Canada will have hotter and drier summers, warmer winters, and more precipitation to fall as rain rather than snow. Conversely, Bruce et al. (2000) predict a slight decrease in precipitation in the southern Maritime Provinces.

Parameter	1980s	2020s	2050s	2080s
Temperature- Annual	5.8	6.9 ± 0.4	8.0 ± 0.6	9.2 ± 1.0
Winter	-5.6	-4.5 ± 0.6	-3.2 ± 0.8	-1.9 ± 1.2
Spring	3.9	4.9 ± 0.5	6.0 ± 0.8	7.1 ± 1.2
Summer	16.9	17.9 ± 0.4	19.1 ± 0.6	20.2 ± 1.0
Autumn	7.9	9.0 ± 0.4	10.1 ± 0.6	11.3 ±1.0
Precipitation - Annual	1204.0	1232.3 ± 34.4	1239.0 ± 38.9	1272.9 ± 53.0
Winter	333.4	346.5 ± 12.1	353.1 ± 16.5	370.5 ± 19.9
Spring	285.2	293.9 ± 12.0	298.5 ± 15.5	309.5 ± 20.7
Summer	261.5	266.1 ± 15.5	263.8 ± 19.2	264.3 ± 32.3
Autumn	323.8	326.4 ± 14.6	324.3 ± 15.9	329.8 ± 26.4
Δ Intensity Short Period Rainfall (%)	0	5	9	16

Table 1.1 Annual changes in temperature and precipitation at Truro predicted by Richards and Daigle (2011).

A study on global warming and precipitation in the United States reports that snowstorms and rainstorms have already become 30% more frequent and more severe than in 1948, producing 10% more precipitation, on average (Madsen and Willcox, 2012). Of particular note to Atlantic Canada is the reported 85% increase in frequency of extreme rainfall and snowfall events in New England, meaning that a storm that used to occur every 12 months now occurs on average every 6.5 months. Singh et al (2013) also predict an increase in precipitation amounts and frequency in coastal areas of the Northeastern United States, and Toreti et al. (2013) use high resolution global climate models to predict a significant intensification of daily precipitation extremes for all seasons.

Studies of streamflow patterns during the last 50 years show that maritime rivers in the Atlantic provinces have been experiencing lower summer flows, but higher flows in early winter and spring (Whitfield and Cannon, 2000; Zhang et al., 2001). Streamflow is expected to increase with temperature and precipitation in the Atlantic region (Najjar et al., 2000), and spring flood could become more common due to changes in late-winter early-spring precipitation patterns (Berrang-Ford and Noble, 2006).

2 Methods

A preliminary hydrodynamic model of the watershed and hydrology within the Indian Brook community was completed in Phase I. This required the acquisition of lidar, a remote sensing method using a laser ranging system on an aircraft to survey high resolution topography, the deployment of multiple field instruments, several field surveys, and the development of a high resolution surface and elevation model for Indian Brook and surrounding area. For Phase II the modelling was completed. This section summarizes fieldwork instrumentation, presents field data, and describes the hydrodynamic modelling.

2.1 Field Work

2.1.1 Phase II Instrumentation Summary

Table 2 documents the fieldwork completed during Phase II in Indian Brook and Figure 2.1 through Figure 2.4 show locations and photos of the instrumentation used in Phase II. Table 3 summarizes the deployment records of field instrumentation used in Phase II.

At the beginning of Phase I, a water depth sensor was deployed at a stream near Indian Brook to continuously measure the stage or height of water in the stream. The sensor was installed during a high water event and was exposed to the air once the water level reduced, and did not record base flow conditions during the majority of the deployment. Once this was determined, a replacement sensor was deployed at a lower level at the same location However, the bridge where these sensors were deployed (referred to as Bridge 1) was replaced by NS Department of Transportation and Infrastructure Renewal and the sensor location had to be changed in early September 2013. A suitable site was found on one of the tributaries draining Indian Brook and the sensor was re-installed at the Indian Road Bridge over Indian Brook, upstream of the reserve (Figure 2.3, Bridge 2). A field visit to download the water level data on February 4, 2014 revealed that the sensor, which was encased in ice, had ceased data collection on January 6, 2014; it was replaced with a sensor that has been collecting data in the river since that date.

The flow measurements and survey grade GPS measurements of the water level were used to build rating curves which relate stage to flow. This information was critical to calibrate and validate a hydrologic model for the system, and is discussed in detail in Section 2.3 on the hydrodynamic model.

In Phase I, a weather station was deployed at Robinson Road in Indian Brook to measure atmospheric conditions (precipitation, temperature, wind, etc.) and was used for model input into the watershed runoff model (Figure 2.4). Other fieldwork involved the identification and measurement of culverts and bridges that represent restrictions for the river channel (Figure 2.5). Stream channel surveys were also conducted, along with GPS measurements of the roadbed above the culverts.

MI'KMA'KI All Points Services hired a surveyor to collect water levels at culverts and document flood conditions during the project (Figure 2.6 and Figure 2.7). The data provided by the surveyor was used to assist in model validation.

Date	Flow measurements	RTK GPS collection	Photos	Notes
06/13/2013	Bridge 1	Yes	Yes	Watershed, area culvert, and flood area inspection with band; installed stage sensor (Solinst) at Bridge 1. Fairly high water. Installed weather station.
60/25/2013	Bridge 1.	Yes	Yes	Area culvert inspection and measurement
07/12/2013	Bridge 1	Yes	Yes	Installed replacement stage sensor at Bridge 1
07/17/2013	Bridge 1	No	No	Flow measurements
07/31/2013	No	No	Yes	Culvert inspection
09/04/2013	Bridge 1	Yes	Yes	GPS water level measurements throughout the watershed. NOTE: New bridge under construction.
09/09/2013	No	Yes	Yes	Removed stage sensors at Bridge 1. Pressure sensor data downloaded.
09/13/2013	No	No	No	Installed stage sensor at Bridge 2
09/24/2013	Bridge 2	Yes	No	Measured stage and flow, and surveyed GPS water level.
10/10/2013	No	No	No	High Water Mark seminar
12/05/2013	Bridge 2	No	Yes	High water measurements and culvert inspection following high water event
01/14/2014	Bridge 2	Yes	Yes	Watershed, area culvert, and flood area inspection with band
02/04/2014	No	No	Yes	Bridge 2 Stage Sensor data downloaded in icy conditions
05/15/2014	Bridge 2	No	Yes	Flow measurements taken at Bridge 2
10/09/2014	Bridge 2	No	No	Flow measurements taken at Bridge 2
10/20/2014	No	No	No	Stage sensor downloaded at Bridge 2
11/18/2014	Bridge 2	No	Yes	Flow measurements taken at Bridge 2
1/20/2015	No	Yes	No	Attempted to download stage sensor at Bridge 2 in icy conditions, RTK measurements taken
2/20/2015	No	No	No	QGIS Workshop

Table 2.1 Summary of visits to Indian Brook during Phase II, or related to Phase II.

Sensor	Location	Data Collection Started	Data Collection Ended
Stage Sensor Solinst Levelogger	Bridge 1	June 13, 2013 19:45 UTC	September 9, 2013 16:00 UTC
Atmospheric Pressure Sensor Solinst Barologger	Bridge 1	June 13, 2013 20:15 UTC	September 9, 2013 16:15 UTC
Stage Sensor Hoboware Pressure Sensor	Bridge 1	July 12, 2013 19:45 UTC	September 9, 2013 16:30 UTC
Hoboware Weather Station	Robinson Road	June 13, 2013 15:45 UTC	Active
Stage Sensor Solinst Levelogger	Bridge 2	September 13, 2013 22:00 UTC	January 6, 2014
Atmospheric Pressure Sensor Solinst Barologger	Bridge 2	September 13, 2013 22:00 UTC	May 15, 2014
Stage Sensor Hoboware Pressure Sensor	Bridge 2	January 14, 2014	Active

Table 2.2 Field instrument deployment summary. When the barologger at Bridge 2 was removed, the pressure data required for compensating the water level data was obtained from the weather station.

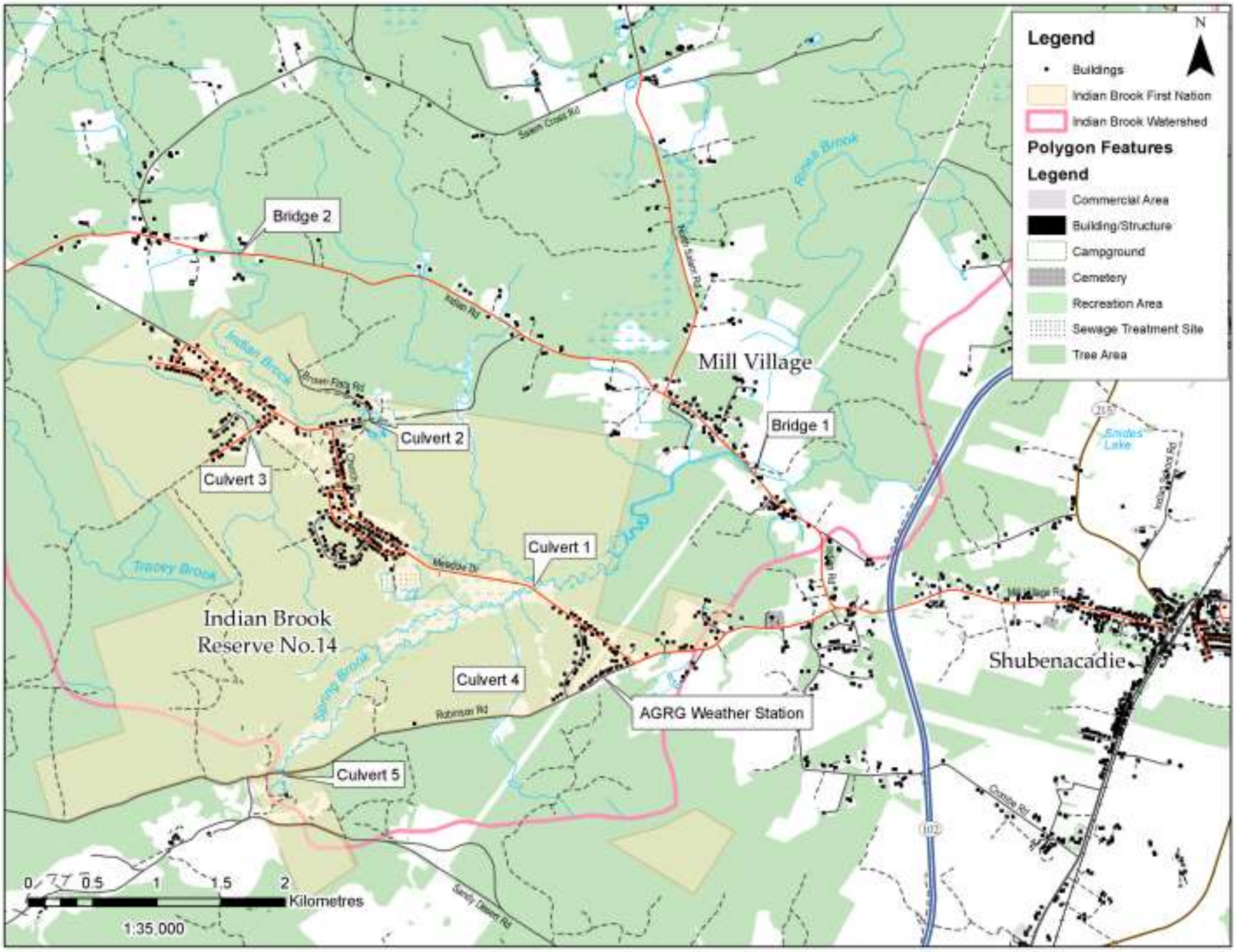

Figure 2.1: Map of Indian Brook showing location of AGRG field instrumentation: the weather station, and the pressure sensor locations.

Figure 2.2: Map and photographs of the Stage Sensors and the first barologger at Bridge 1 on Indian Road near Mill Village.

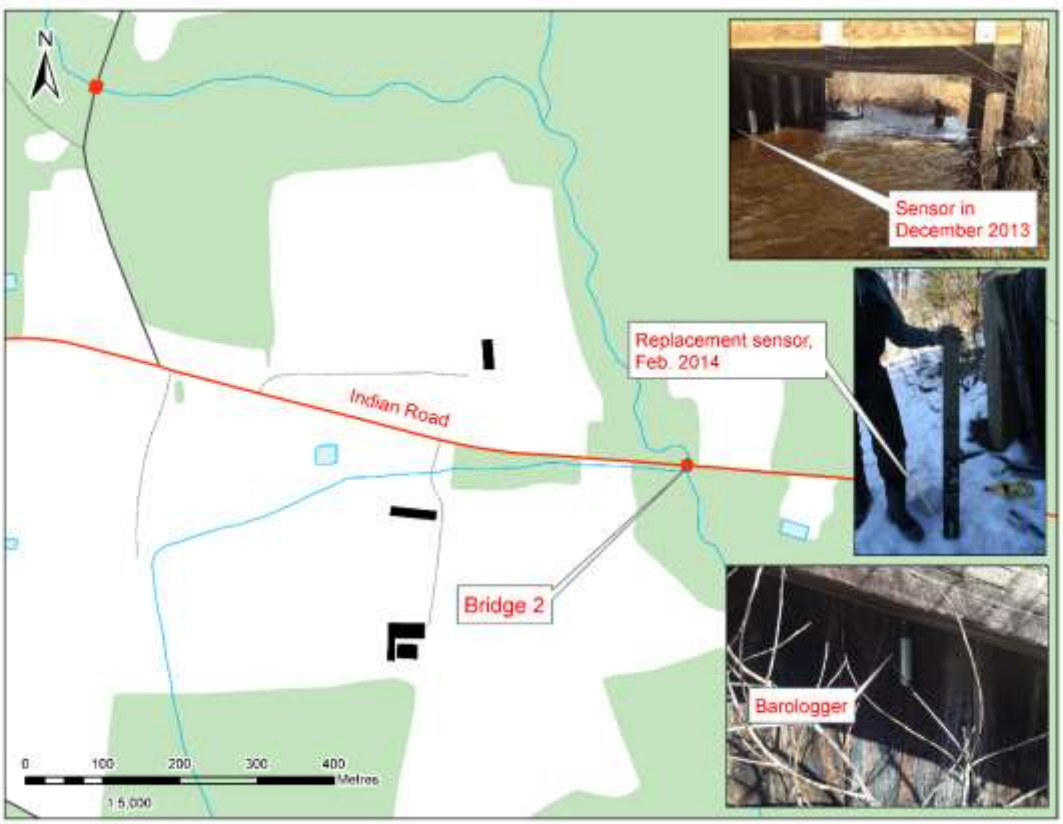

Figure 2.3 Map and photographs of stage sensors and the barologger on Indian Road at Bridge 2.

Figure 2.4: AGRG weather station during deployment on June 13.

Figure 2.5: Locations and photos of culverts shown in **Figure 2.1**.

Figure 2.6 Flooding at Brown Flats Road, culvert 2H on (a) November 28, 2013; (b) December 4, 2013. Map shows location of culverts.

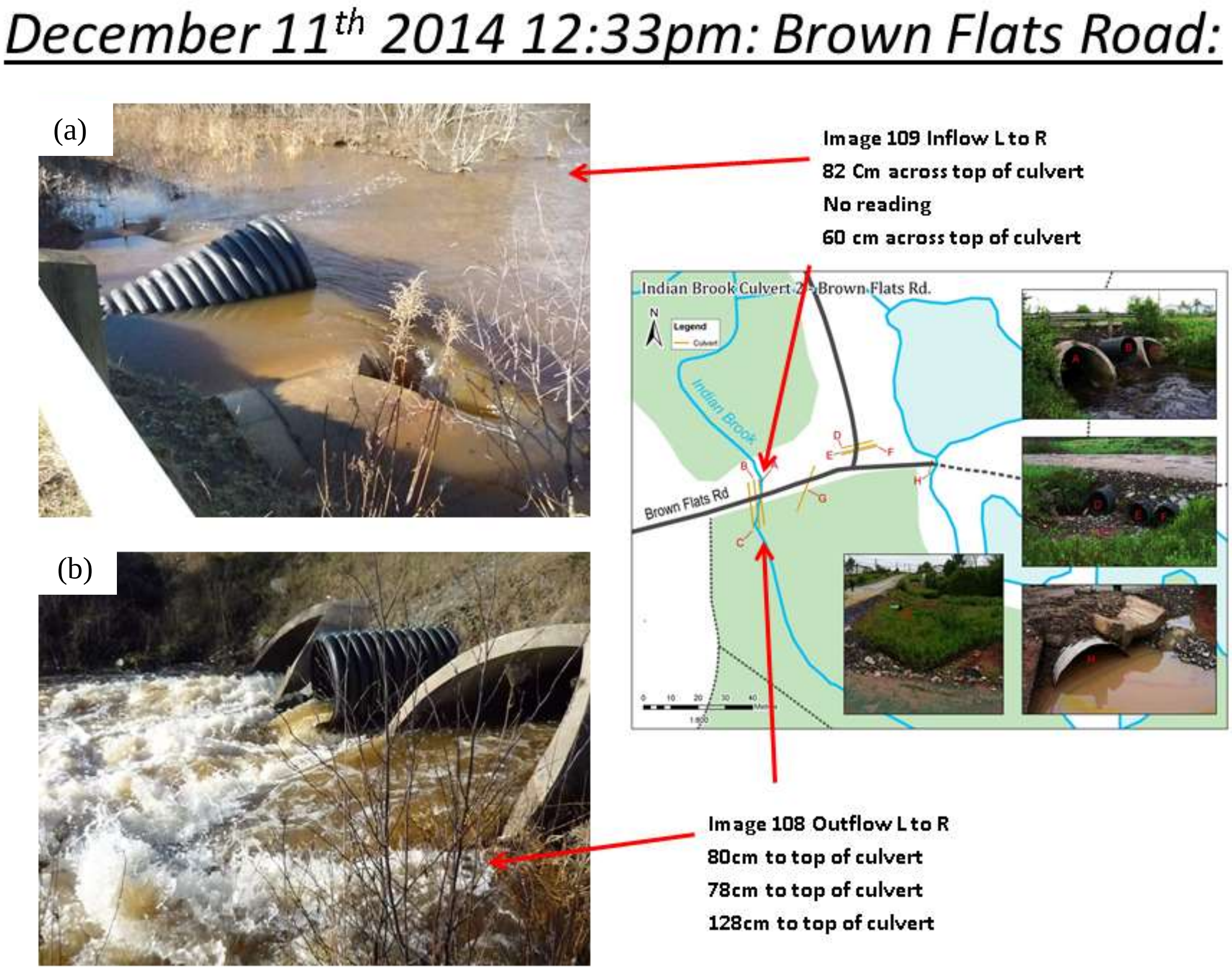

Figure 2.7: Flooding at Brown Flats Road on December 11, 2014 at culvert 2ABC (a) inflow, (b) outflow. Map shows location of culverts.

2.1.2 Data

Figure 2.8 shows the water level at Bridge 1 measured by the replacement sensor during the deployment. Figure 2.9 shows the water level data at Bridge 2 from the beginning of the deployment on September 13, 2013 until the most recent data download on October 20, 2014. Precipitation data from the AGRG weather station highlights the coupling of rainfall events and increased water level at both locations. During the winter of 2014, below freezing temperatures and ice covering the river caused the sensor at Bridge 2 to malfunction, and data between January 6 and February 4, 2014 when the sensor was replaced, were discarded (Figure 2.10).

Figure 2.11 shows data recorded at the AGRG weather station on Robinson Road for Nov. 20 – Dec. 25, 2013 highlighting the flood events documented in Figure 1.2 and Figure 1.3; Figure 2.12 shows data recorded at the

AGRG weather station for Nov. 15 – Dec. 15, 2014 highlighting the flood events documented in Figure 1.5 and Figure 1.6. Complete AGRG weather station data is found in Appendix A: Weather Station Data.

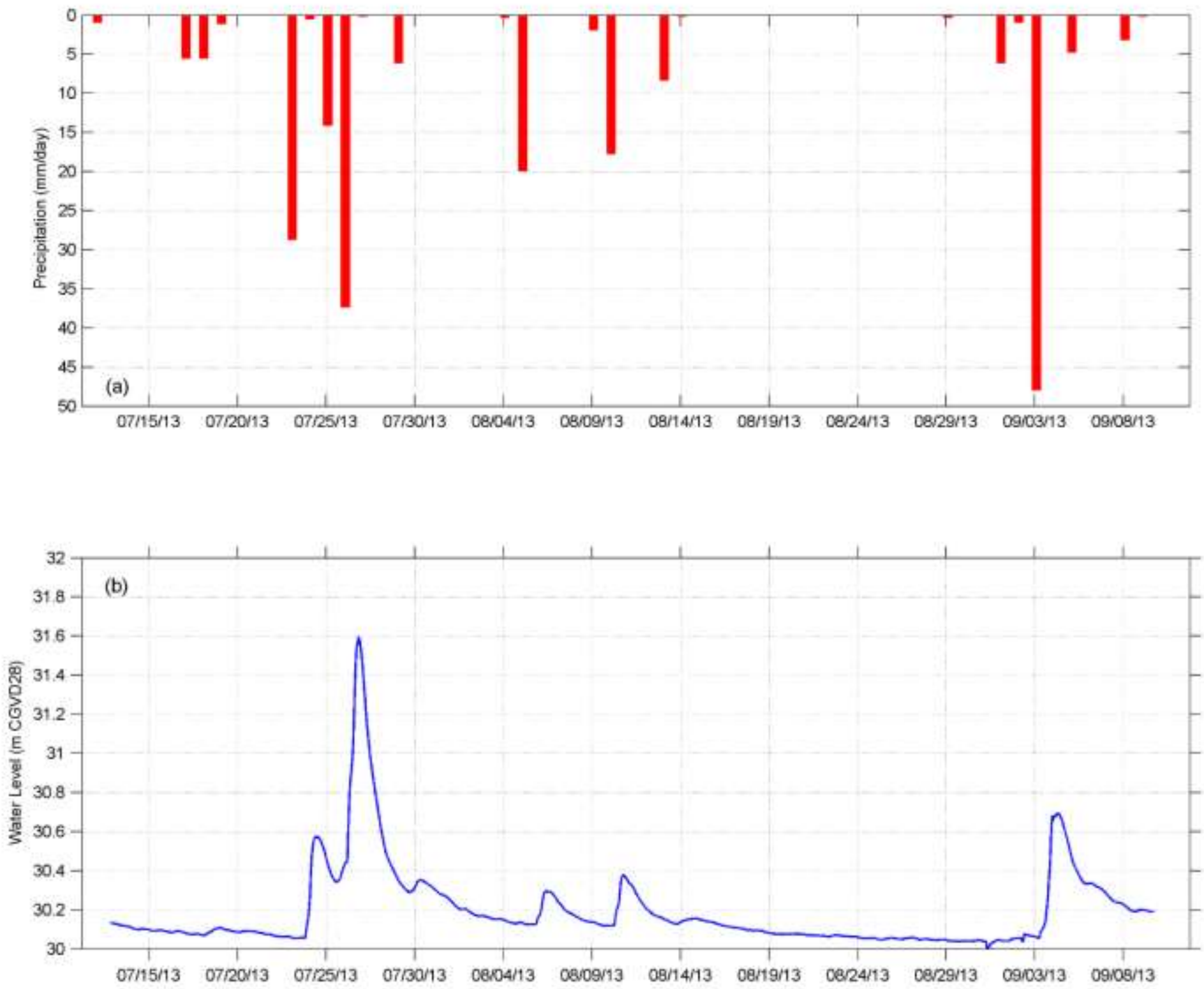

Figure 2.8: (a) Daily precipitation at AGRG Robinson Road weather station; (b) water levels recorded at Bridge 1 by the replacement sensor.

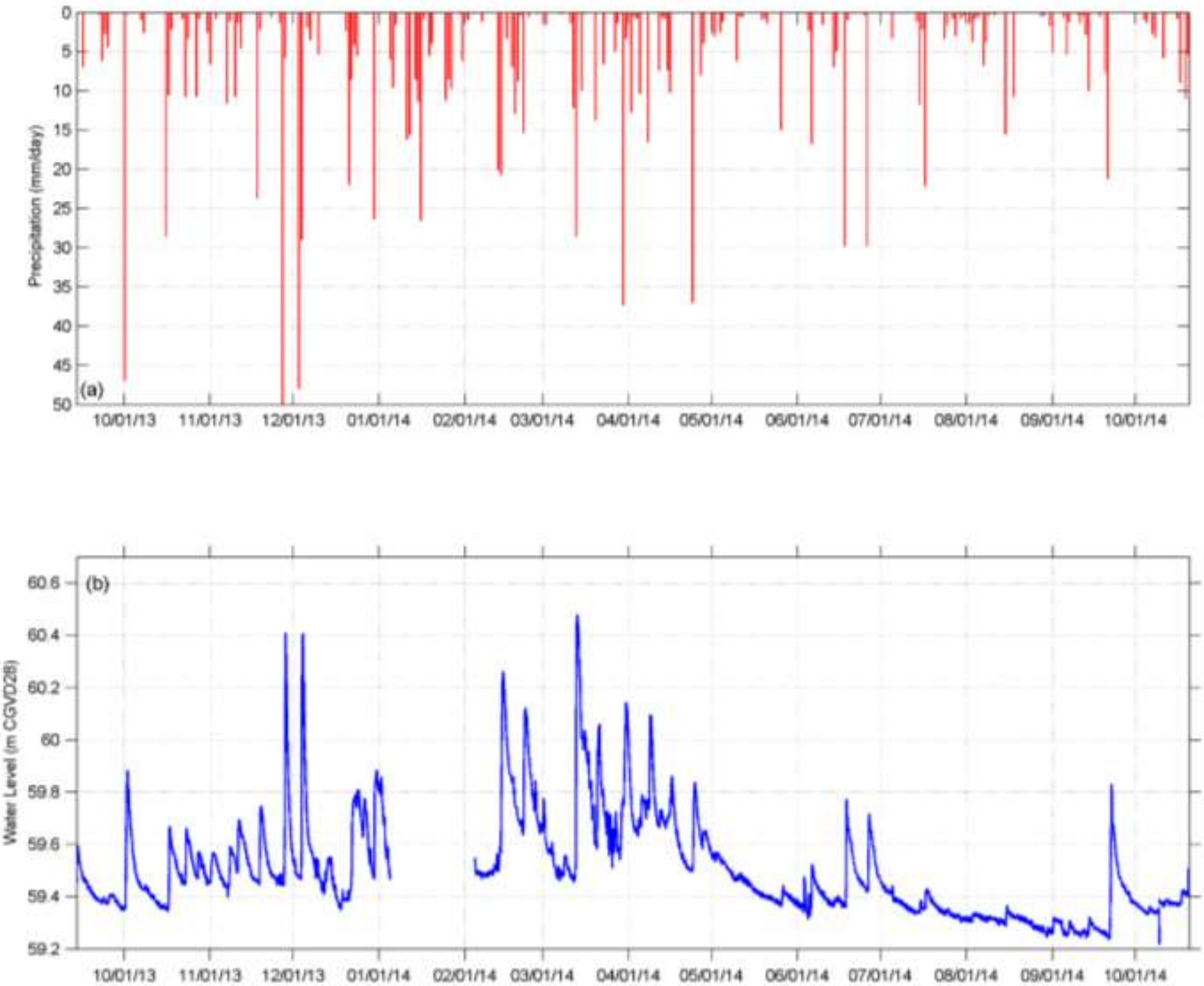

Figure 2.9 (a) Daily precipitation at AGRG Robinson Road weather station; (b) water levels recorded at Bridge 2.

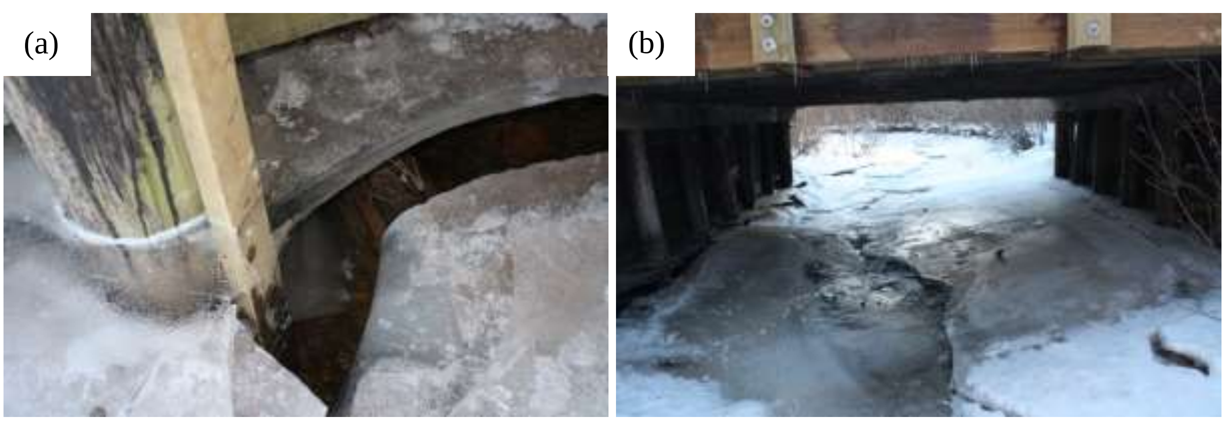

Figure 2.10 (a) Stage Sensor under the ice at Bridge 2 on February 4, 2013; (b) Bridge 2 iced over on February 4, 2013.

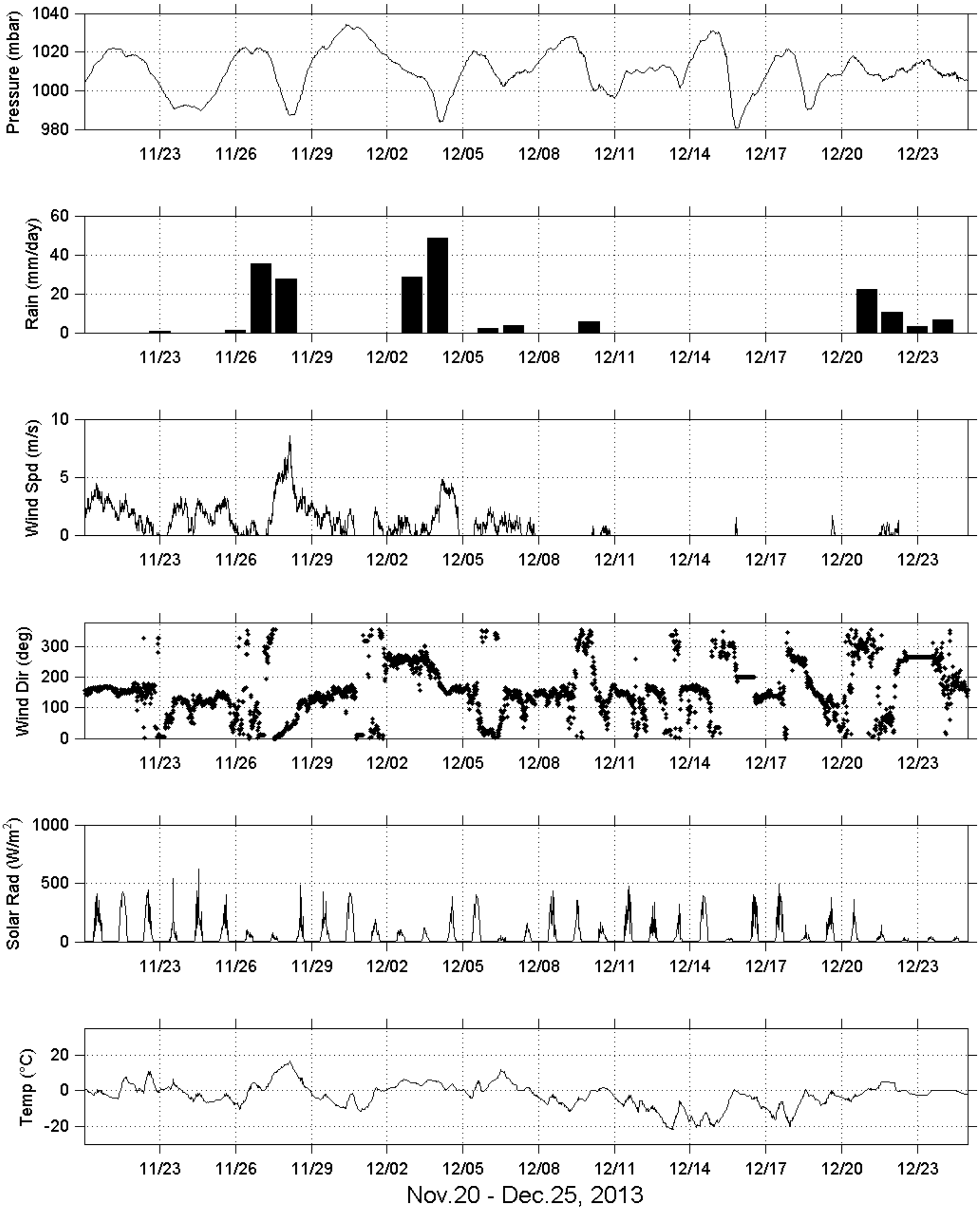

Figure 2.11: Meteorological data recorded at Robinson Road weather station from November 20 to December 25, 2013. The heavy rainfall events of November 28 and Dec 3-4 are evident in the observations.

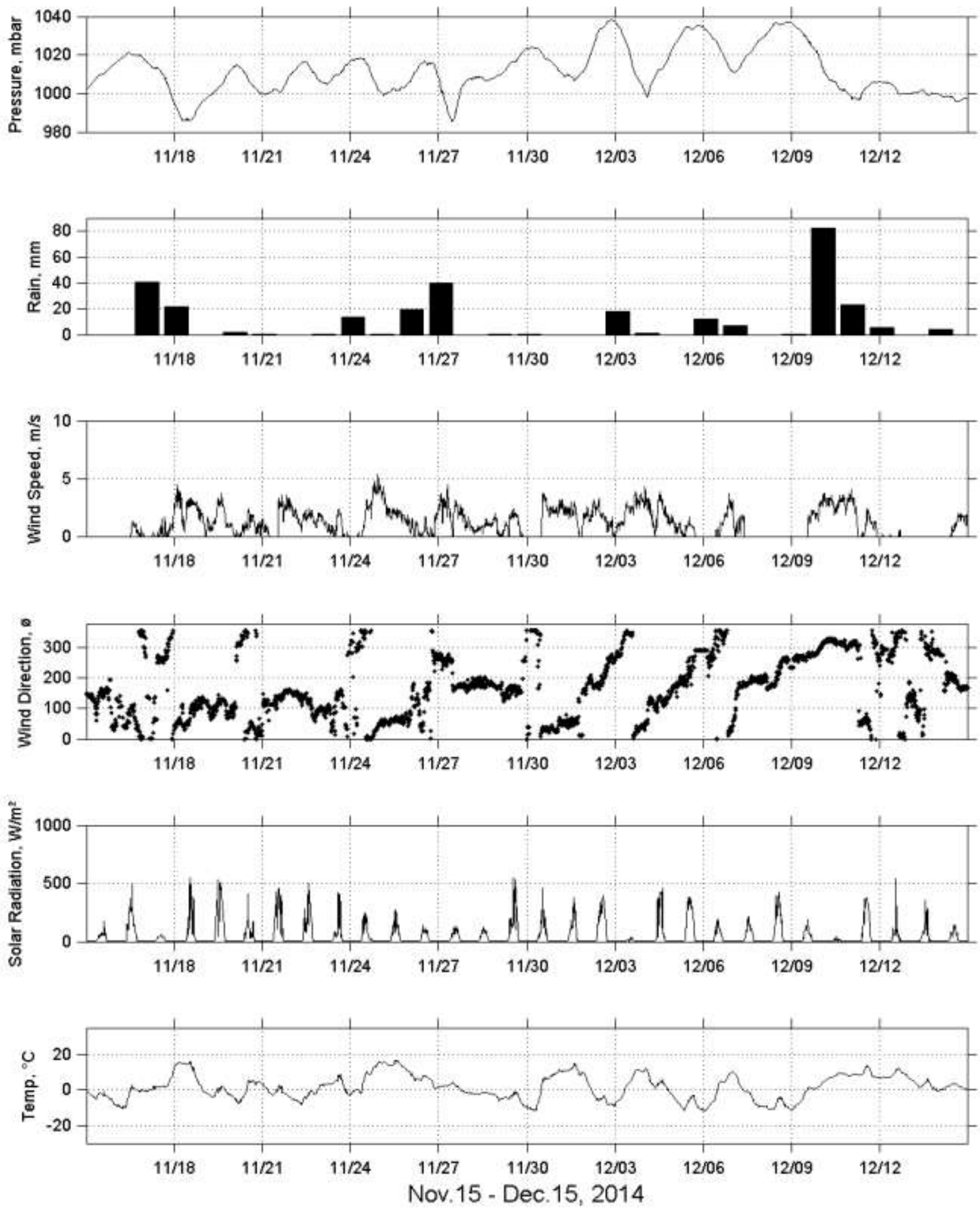

Figure 2.12 Meteorological data recorded at Robinson Road weather station from November 15 to December 15, 2014. The heavy rainfall events of November 17-18 and 26-27, and Dec 11-12 are evident in the observations.

2.2 Hydrodynamic Modelling

We used a coupled one-dimensional and two-dimensional depth averaged shallow water hydrodynamic modelling system based on the incompressible Reynolds averaged Navier-Stokes equations, Mike 11 and Mike 21 by the Danish Hydraulic Institute (DHI). Flood simulations were conducted on a lidar derived two-dimensional topography with integrated culvert structures and river channel geometry calibrated for surface roughness. The model uses rainfall and temperature data from the weather stations to drive the model and simulate the extent of flooding over the lidar mesh following heavy rainfall events. The flood model is validated and calibrated using water depth sensors deployed in the river system, periodic river flow measurements, and high precision RTK GPS river stage measurements all collected throughout the project.

2.2.1 1-D Hydrodynamic Model

2.2.1.1 DEM Preparation

The 1 m lidar DEM presented and described in the Phase I report was integrated with 20 m resolution elevation data from the Nova Scotia Topographic Database (NSTDB) to produce a cohesive elevation model for the entirety of the Indian Brook watershed. The 1 m resolution lidar data was given preference where available and the 20 m data was used outside of the lidar zone (Figure 2.14).

The Indian Brook watershed extent was calculated using a suite of hydro tools within the ESRI ArcMap 10 software package which relied heavily on elevation data obtained from the 1 m lidar-based DEM. The tools were used to simulate theoretical drainage between adjacent cells based on elevation differences to form watershed boundaries and river networks based on accumulated flow calculations. The DEM was appropriately prepared by lowering elevation values where culverts or bridges existed to ensure proper drainage characteristics between adjacent cells. In the correction process, each structure was removed from the DEM and the lowest surrounding elevation value was used for the gap. The catchments draining into Bridge 1 encompassed an area of 47.95 km^2, while catchments draining into Bridge 2 encompassed 15.03 km^2 (Figure 2.14). Catchment areas and land cover drainage characteristics were used as an input parameter within the Mike 11 Rainfall-Runoff model.

The Mike11HD model requires accurate stream and floodplain topography in order to simulate the flow of water through the system. The river network was sectioned into unique branches with length (chainage) measured in meters (Figure 2.14). Each branch was then linked with its appropriate catchment in order to create a stable network input for simulations. Mike11HD does not continuously calculate flow along river branches, rather, it calculates flow at defined cross-sections in order to transfer flow between cross-sectional distances where equations are based on the conservation of momentum principle. Cross-sections were manually digitized across river branches and flood plains perpendicular to the direction of flow. Cross-sections were roughly spaced at 300 m intervals along river branches while ensuring that a cross-section was drawn at the start and end chainage of each river branch. Cross-section width was dependent on topography and was ensured to capture potential flood plains during significant flooding events. Elevation was extracted from the hybrid DEM and applied to each cross-section. Conveyance and water level were calculated for each of the two-dimensional cross-sections based on theoretical water elevation within the cross-section at 1 cm increments. Cross-section topography and conveyance potentials were stored within the final cross-section input file for hydrodynamic (HD) simulations.

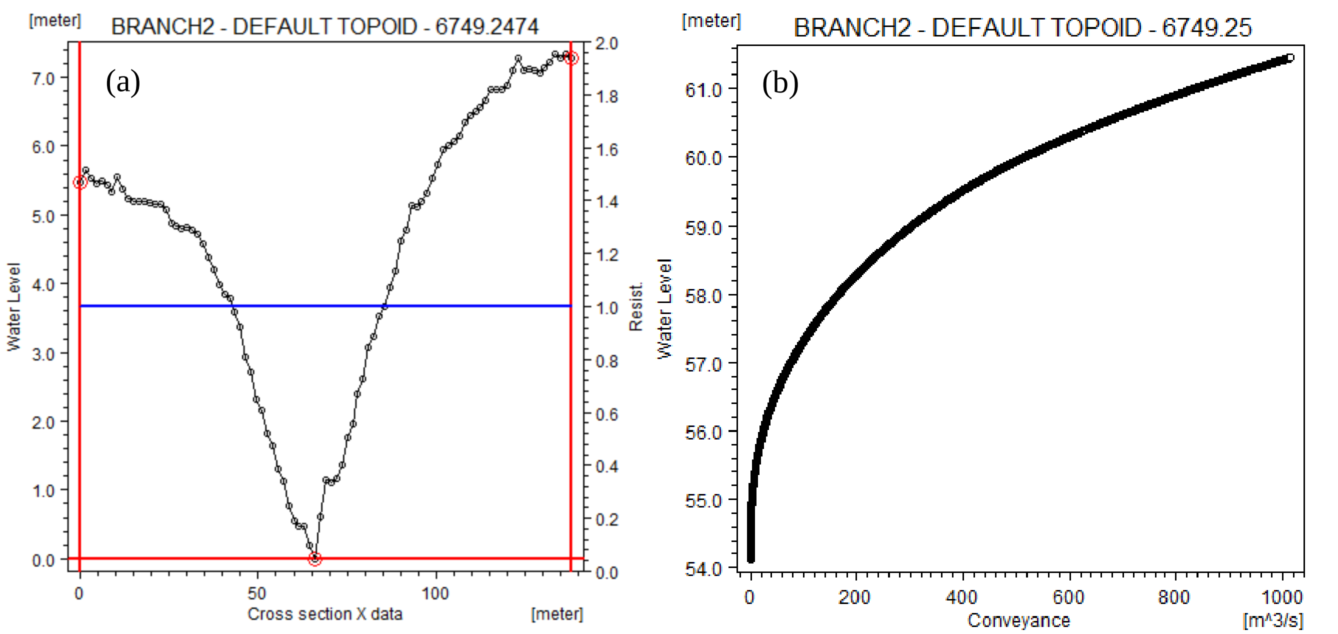

Figure 2.13 (a) Branch 2 cross-section oriented perpendicular to flow. Elevation data along the length of the cross-section were extracted from the DEM. The minimum possible water level corresponded to the minimum elevation within the cross-section (horizontal red bar) and the maximum flood banks of the cross-section were drawn at the left and right end points (vertical red bars); (b) Potential conveyance was calculated based on water level increments within the possible flood area.

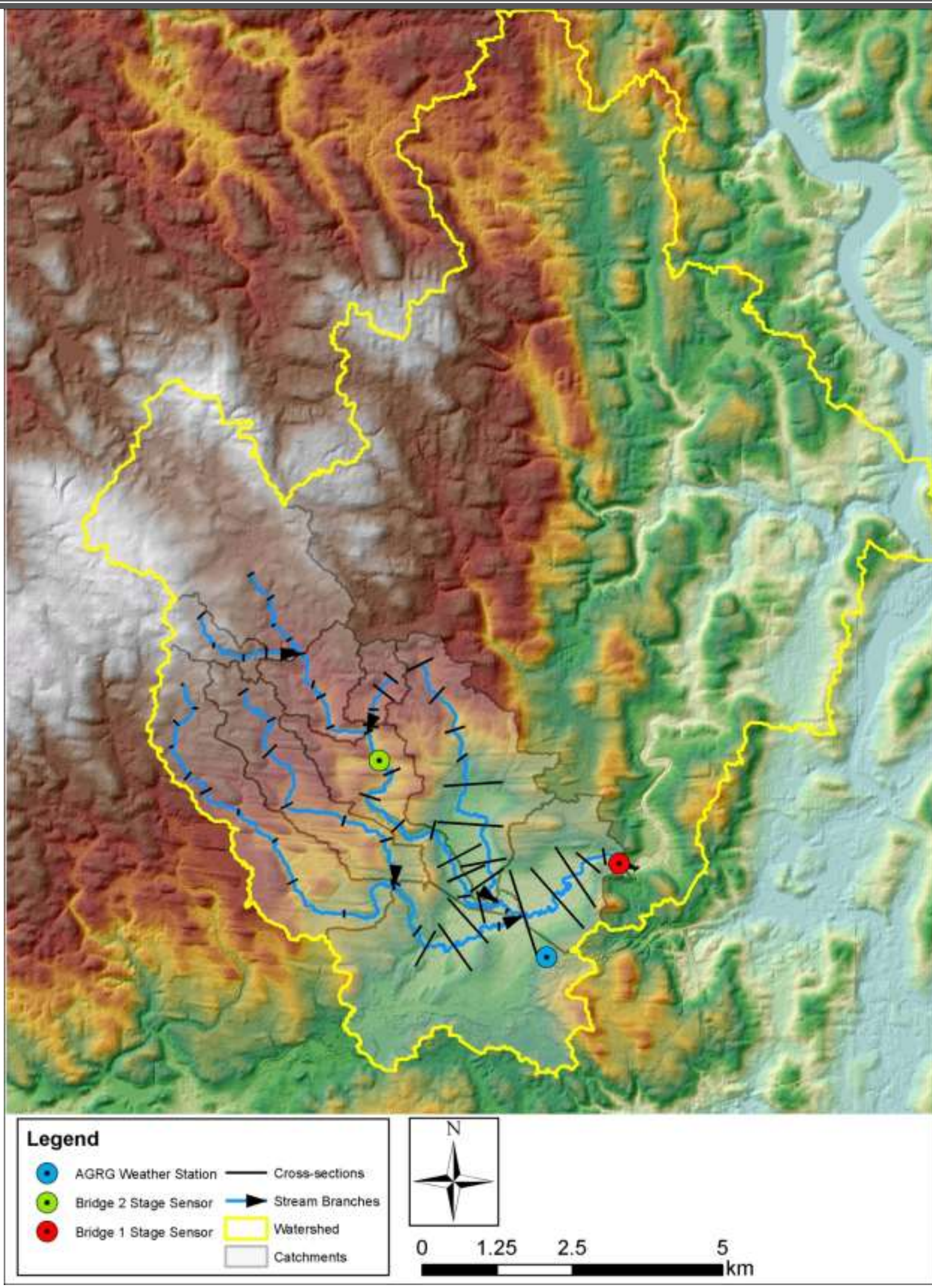

Figure 2.14: Hybrid digital elevation model of Indian Brook watershed generated using 20 m resolution NSTDB elevation data and 1 m resolution lidar data showing AGRG weather station, Bridge 1, Bridge 2, catchment areas, stream branches and cross-sections used in the 1-D hydrodynamic model.

2.2.1.2 Rainfall Runoff Model

The Indian Brook rainfall runoff model was driven by a Rainfall Dependent Inflow and Infiltration model (RDII) within the Mike11 software suite, by DHI. The rainfall runoff model is a generalized watershed model that simulates the discharge of water by quantifying routing times and storage zone capacities. The model is forced with observed precipitation and evapotranspiration, a measurement derived from daily temperature minima and maxima indicating the amount of water entering the air from evaporation and plant transpiration, using data from the AGRG Weather Station. The water pressure recorded by the stage sensors deployed at Bridge 1 and 2 is converted to stage elevations or water levels by measuring the offset between the sensor GPS position and the recorded depth. Variances in barometric pressure are compensated for using readings from the barologgers installed on the bridges or the AGRG weather station.

Rating curves were calculated for Bridge 1 and Bridge 2 in order to relate water level (stage) to discharge. The rating curve for Bridge 1 was calculated during Phase I, but the Bridge 2 rating curve was re-calculated for Phase II using additional water level and flow data. The rating curve uses observed flow measurements that were taken using a Valeport electromagnetic (EM) flow meter or a Valeport suspended impeller flow meter depending on safety requirements related to river stage. The method of flow calculation was the same for both units; flows were recorded under the bridge perpendicular to the river orientation at a 0.5 m sampling interval. Velocity was measured for each of the 0.5 m columns using the average of 30 second sampling intervals which recorded 1 sample per second. For depths less than 50 cm, water velocity was measured at the 60% depth (in a water depth of 10 cm, a velocity measurement was recorded at 6 cm). For depths greater than 50 cm, water velocity was calculated using the average of a 20% depth measurement and 80% depth measurement. Velocity was averaged over each of the 0.5 m columns to produce an average flow measurement. Total discharge was calculated by summing flows from each of the 0.5 m columns. The coordinates of the bridge deck and rail were surveyed using a differential RTK GPS setup to within 3 cm of vertical precision. River stage elevations were calculated by measuring the offset between the bridge rail and the water surface during each of the flow measurements. The rating curves and equations for each bridge are shown in Figure 2.15. The discharge rating curve was a best fit line to the observed river flow and stage data. The line is ideally fit with flow observations conducted during different times under different flow conditions, and more high flow measurements result in a rating curve that we have more confidence in for extreme event modelling. The rating curve for Bridge 1 presented here is the same as the rating curve presented in the Phase I report, but the Phase II rating curve has been updated with more observations. Unfortunately, the dry summer provided few opportunities for high flow measurements, but a few higher flow observations were recorded in the fall, allowing for the calculation of a much improved Bridge 2 rating curve.

The equation for discharge resulting from the rating curve allows us to use the continuous water level stage data recorded by the sensors to produce a time series of discharge at each bridge; these are used as model calibration and validation for the Rainfall-Runoff model.

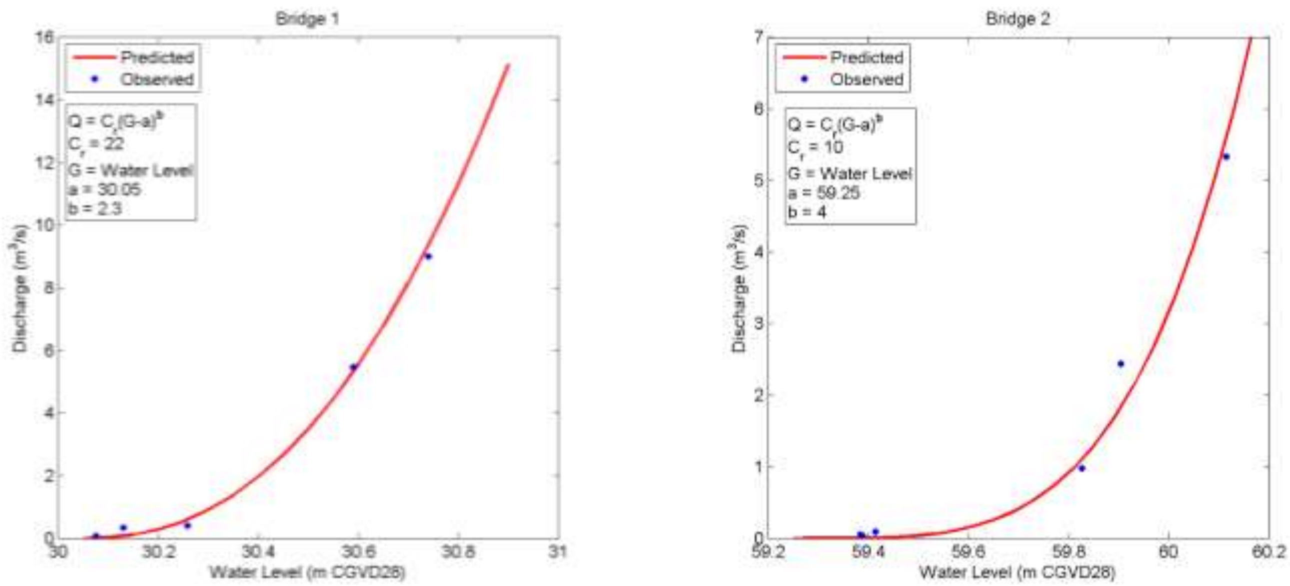

Figure 2.15: Rating curve derived from measured water level and discharge at (a) Bridge 1 and (b) Bridge 2. Note the different scale of the y-axis in (a) and (b), showing that more high flow observations were recorded at Bridge 1 than at Bridge 2.

The Rainfall Runoff models for each Bridge were calibrated using an iterative process of fine-tuning watershed infiltration/runoff parameters until the modelled discharge matched the observed (Figure 2.16 and Figure 2.17). The Bridge 1 model predicted discharge well for a high flow event on September 5, but grossly under predicts an event on July 27 (Figure 2.16). Although the precipitation recorded at the AGRG weather station does indicate a rainfall event on that date, the Environment Canada weather radar for July 27 indicates that the heaviest rainfall passed through the north of the watershed, missing our weather station but depositing heavy rain into the watershed, and thus into the river system. Thus, the observed discharge data reflects a precipitation event, but the rainfall data being used to force the modelled discharge under-predicts this rainfall event since it is located within the community in the south of the watershed (Figure 2.14).

The Bridge 2 model performs well during the November 28 and December 4, 2013 storm events (Figure 2.18) as well as during lower flow events. The model predicts the timing of events in winter of 2014 well, but under-predicts their magnitude. The precipitation record does not show high rainfall associated with the high discharge events (e.g. mid-March 2014), suggesting that the high water level events recorded by the sensors were due in part or in whole to melting snow rather than rainfall. Photo documentation of these high water events confirms the presence of snow on the ground during those times (Figure 1.4).

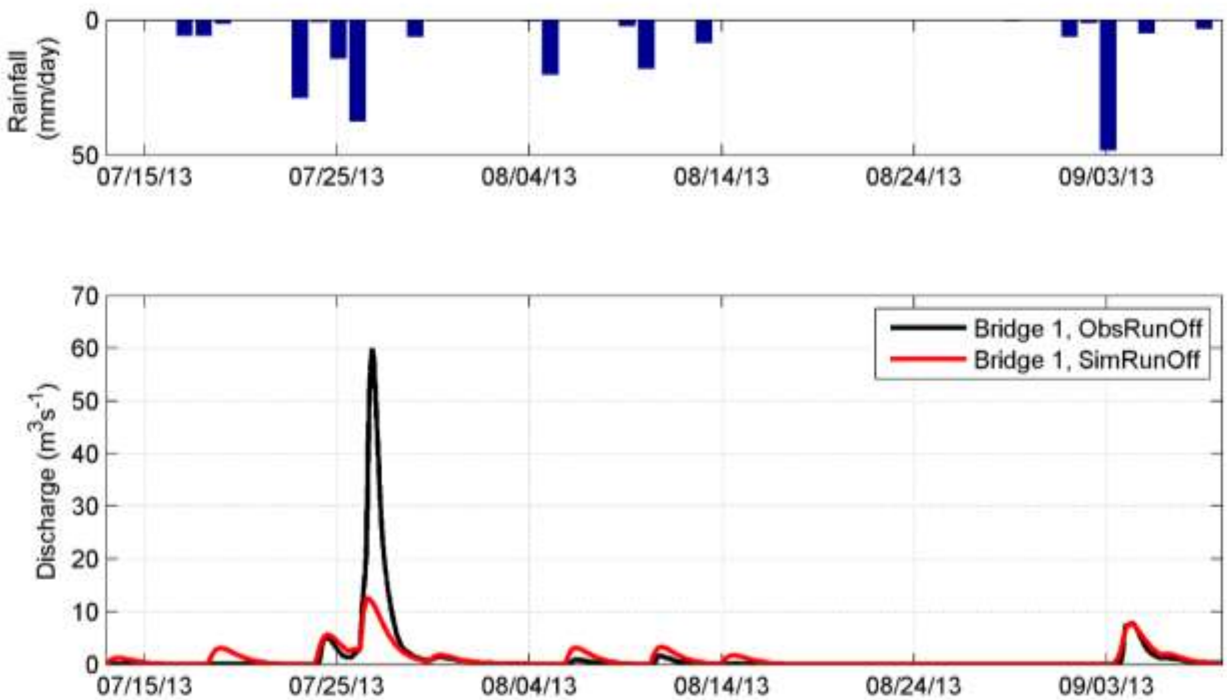

Figure 2.16: Precipitation and river runoff model calibration results for Bridge 1 for its entire deployment.

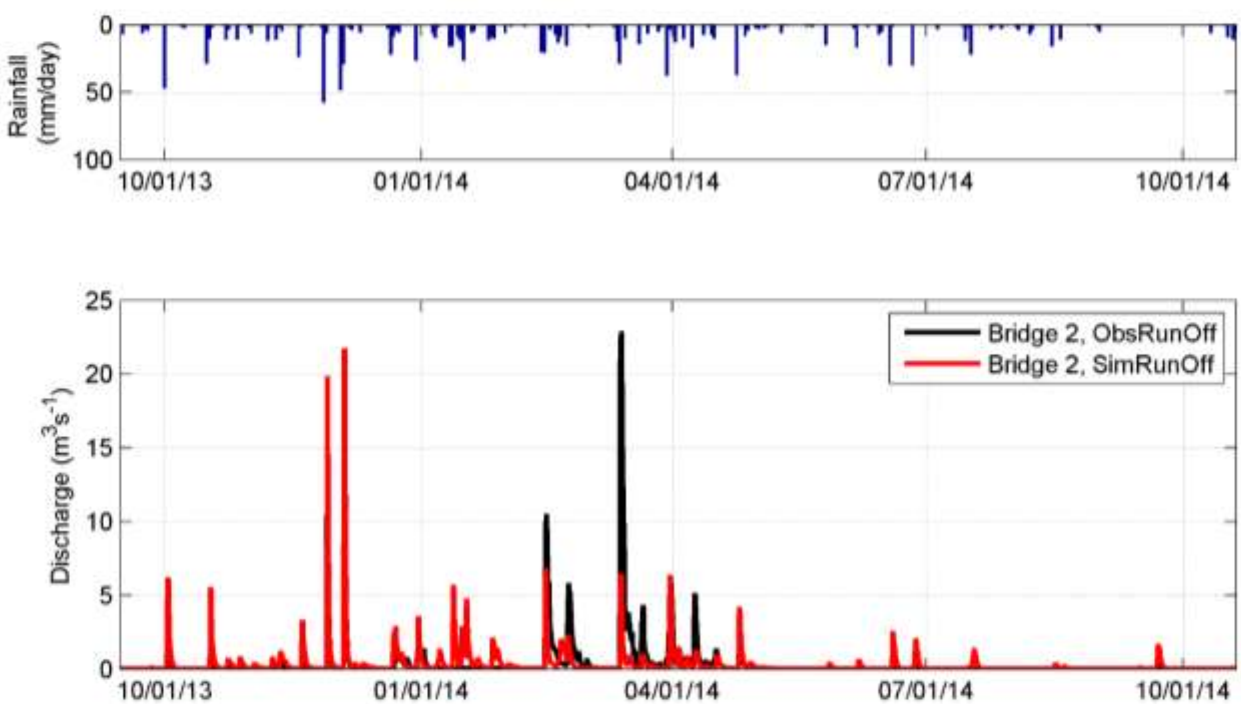

Figure 2.17: Precipitation and river runoff model calibration results for Bridge 2 for its entire deployment.

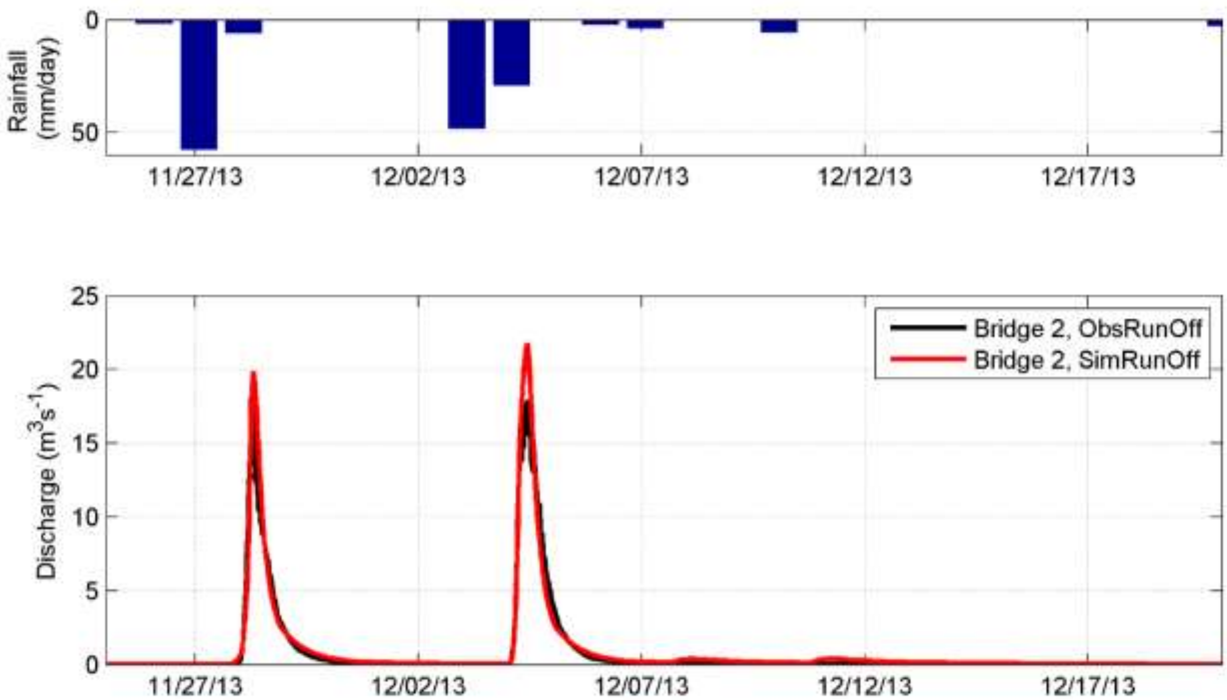

Figure 2.18: Precipitation and river runoff model calibration results for Bridge 2 with time axis restricted to show the November-December 2013 flood events.

2.2.1.3 Hydrodynamic Model

The added benefit of a hydrodynamic model over a generalized rainfall model is the ability to simulate the physical flow of water within a system. Simulating flow allows for the calculation of water elevations at cross-section points along model river branches. One dimensional hydrodynamics were modeled using the Mike11HD component of the Mike software suite by DHI. The hydrodynamic model component required calibrated Rainfall Runoff models for each sub-catchment in the Indian Brook watershed and suitable river cross-sections for conveyance calculations and floodplain delineation (refer to Section 2.3.1.1 on cross-sections). The calibrated rainfall runoff models were used to provide the hydrodynamic model with inflow data after rainfall events. Inflow from catchments is routed to the appropriate river branches by the hydrodynamic model and flow is simulated to the downstream terminus of the river network. The hydrodynamic discharge and water levels were also calibrated against observed discharge records to ensure that flow was being properly routed between cross-sections and that bed resistance values were realistic (Figure 2.19).

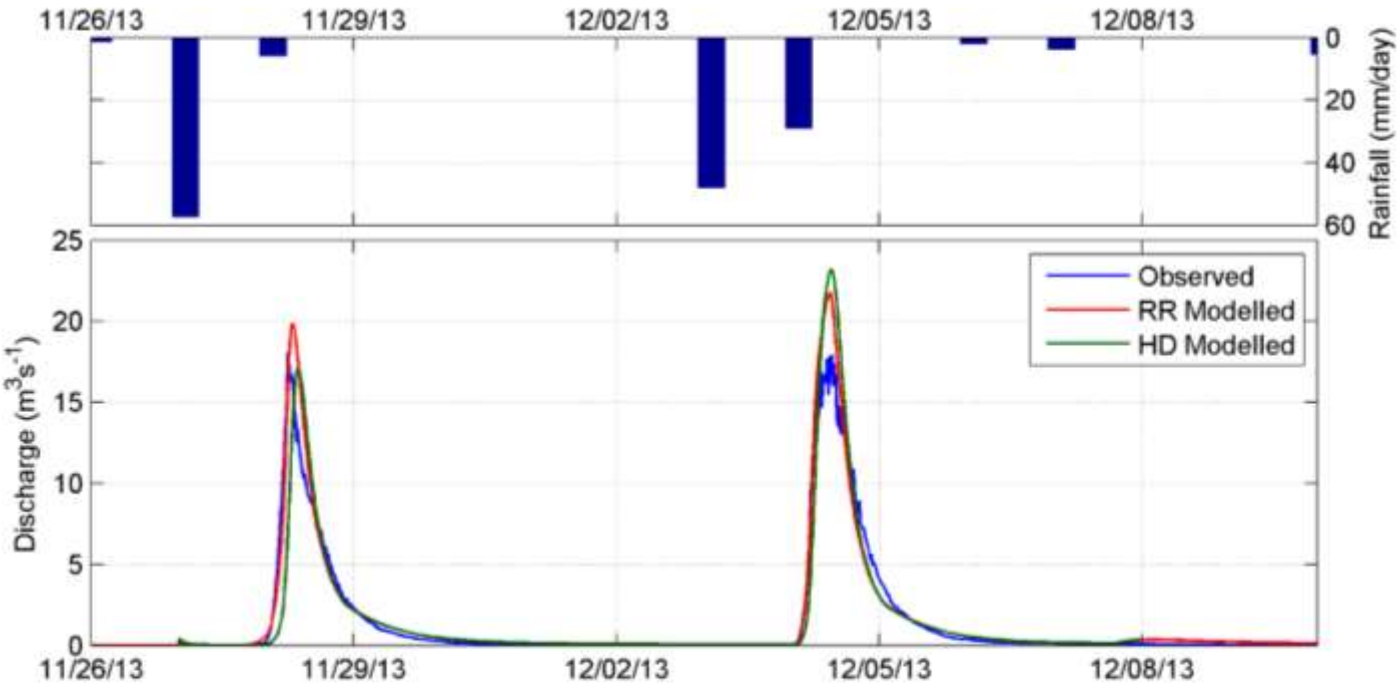

Figure 2.19: Precipitation (top panel); observed runoff at Bridge 2, river runoff model calibration, and hydrodynamic model calibration (lower panel).

2.2.2 2-D Hydrodynamic Model

A more robust two dimensional hydrodynamic model was required to map two dimensional flooding caused by the overtopping of riverbanks represented in the one dimensional model discussed above. The Mike21 software package was used to calculate depth averaged 2-D hydrodynamics over a DEM of the earth's surface. A lower resolution 6 m DEM was built using the 1 m lidar data to stabilize Mike21 calculations and reduce processing time. The 2-D model effectively calculated the transfer of water between adjacent hydrologically connected cells within the model domain (Figure 2.20).

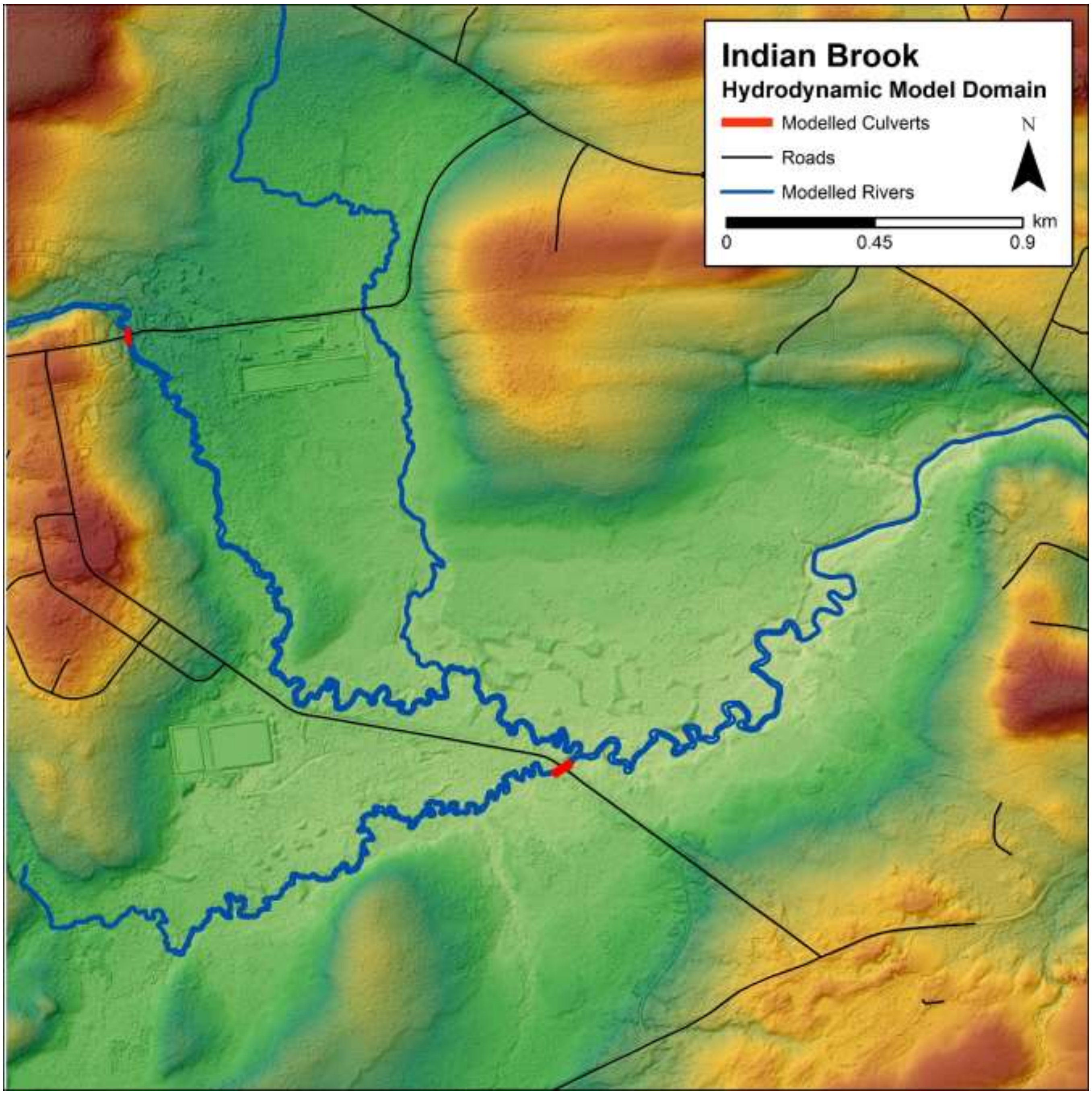

Figure 2.20: Mike21 6 m resolution model domain used in 2-D hydrodynamic modelling.

The developed 1-D hydrodynamic model was linked to the 2-D hydrodynamic model using the MikeFlood software package. The linkage allowed for the transfer of rainfall and stream level data calculated within the 1-D model to be applied to domain of the 2-D model. The linkages between models were formed at the banks of the 1-D stream cross-sections. In the event that flooding caused water to overtop a riverbank the volume of water was transferred to the coincident Mike21 model cell as discharge. Culverts and bridges were modelled using in-situ measurements to ensure realistic conveyance of water through these constriction points which are often the cause of flooding after significant rainfall events (Figure 2.21).

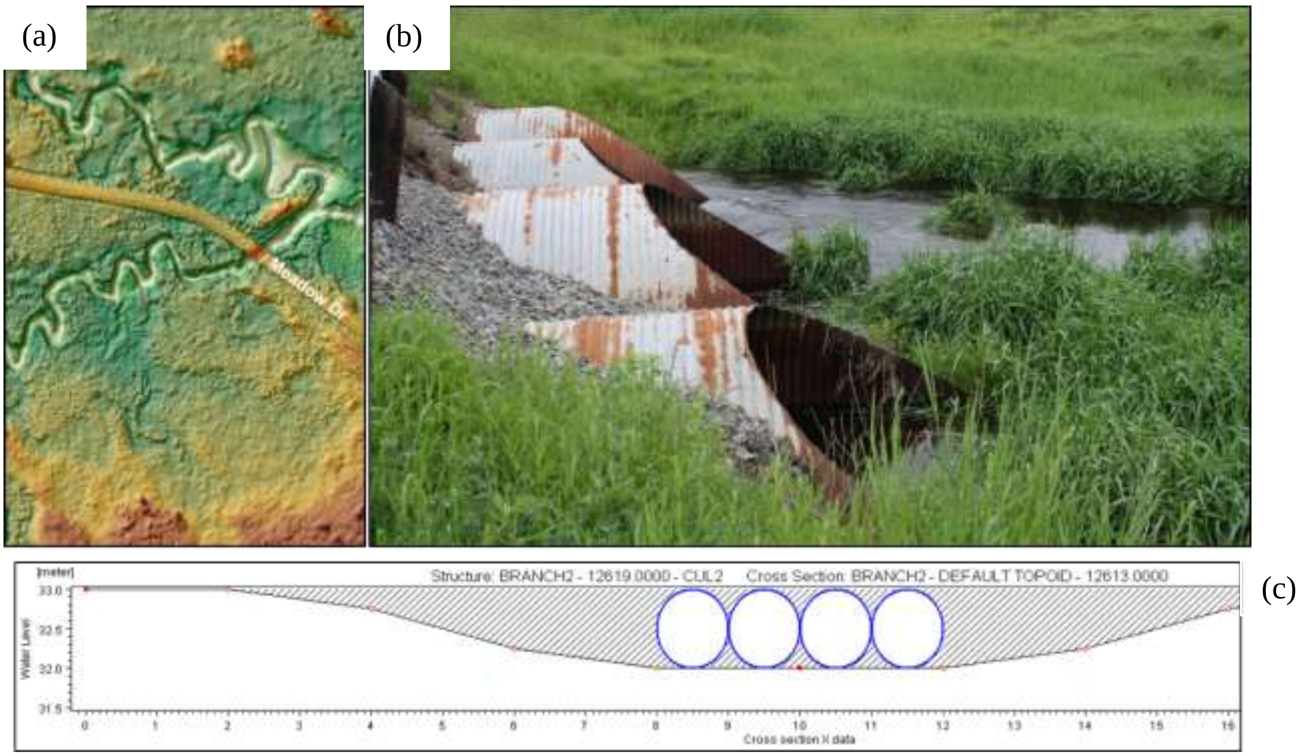

Figure 2.21 (a) Surface model and (b) photos of the four large, partially obstructed culverts 1A,B,C,D on Meadow Drive, the low-lying area prone to flooding; (c) the culverts were digitized and included as a flow impedance within the MikeHD model.

2.3 Model Simulations

Several model iterations were run to simulate changes in environmental and structural inputs that would ultimately change the magnitude and extent of inundation caused by significant rainfall events. For model validation, culverts were added to the hydrodynamic framework to represent their current conditions and realistically simulate the ability of existing culverts to route water over a simulation period in response to observed rainfall. Following validation, the structure of the model culverts was adjusted to create: i) a cleared culvert condition which increased the effective area of the model culverts to their maximum/actual measured dimensions and set resistance values based on engineering specifications; this scenario represents new culverts, ii) an impeded culvert condition that reduced the effective area of the culvert and increased bottom resistance and represents potential deteriorating conditions in the future, iii) a bridge condition which replaced the culverts with bridges that span the same area (Table 2.3).

Condition	Location	Composition	Manning's n	Dimensions (m)	Discharge Area (m^2)
Modelled Culverts (Current Condition)					
	Brown Flats Rd.				
	A	Concrete	0.011	1.8	5.65
	B	Annular PVC	0.024	0.9	2.83
	C	Concrete	0.011	1.8	5.65
	Meadow Rd.				
	A	Helical Corr. Steel	0.026	2	6.28
	B	Helical Corr. Steel	0.026	2	6.28
	C	Helical Corr. Steel	0.026	2	6.28
	D	Helical Corr. Steel	0.026	2	6.28
Cleared Culverts (New Condition)					
	Brown Flats Rd.				
	A	Concrete	0.011	1.8	5.65
	B	Annular PVC	0.024	0.9	2.83
	C	Concrete	0.011	1.8	5.65
	Meadow Rd.				
	A	Helical Corr. Steel	0.021	2.1	6.60
	B	Helical Corr. Steel	0.021	2.1	6.60
	C	Helical Corr. Steel	0.021	2.1	6.60
	D	Helical Corr. Steel	0.021	2.1	6.60
Impeded Culverts (Deteriorating Condition)					
	Brown Flats Rd.				
	A	Concrete	0.026	1.6	5.03
	B	Annular PVC	0.024	0.9	2.83
	C	Concrete	0.026	1.6	5.03
	Meadow Rd.				
	A	Helical Corr. Steel	0.035	1.8	5.65
	B	Helical Corr. Steel	0.035	1.8	5.65
	C	Helical Corr. Steel	0.035	1.8	5.65
	D	Helical Corr. Steel	0.035	1.8	5.65
Bridge					
	Brown Flats Rd.				
	Bridge	Streambed	0.030	5 x 3	15.00
	Meadow Rd.				
	Bridge	Streambed	0.030	9 x 2.5	22.50

Table 2.3: Values used to simulate variations in engineered structure conditions which increased or decreased the potential to convey water effectively within the hydrodynamic model.

In addition to the physical changes, a model condition was developed to simulate increased rainfall intensity due to climate change. Rainfall amounts were increased by 16% in accordance with projections discussed in Section 1.3 (Richards and Daigle, 2012). An increase of 16% changed the total accumulated rainfall from 139.8 mm to 162.2 mm over the model validation period of November 27, 2013 to December 5, 2013 (Figure 2.22). The increased precipitation scenario was simulated using modelled culverts in their current condition as well as culverts replaced with bridges.

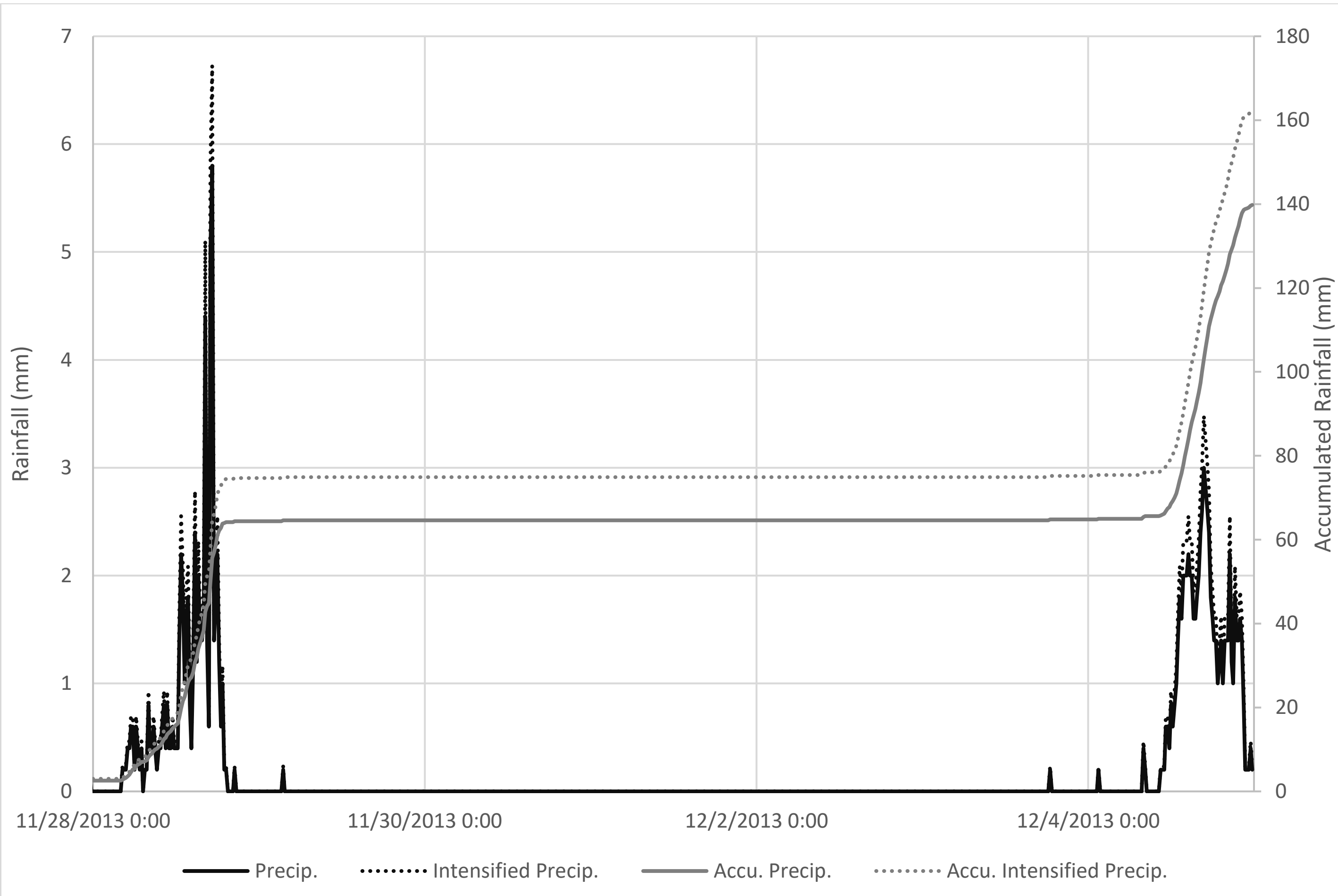

Figure 2.22: Increased precipitation amounts as a result of climate change projections which predict a 16% increase in rainfall intensity.

3 Results

3.1 Model Validation

The 2-D hydrodynamic model was calibrated using in-situ observations from two flood events that occurred between November 27th, 2013 and December 5th, 2013. This calibration event was particularly useful because of the short time period between the two major rain events. The first caused flooding on November 28th, 2013 which only briefly overtopped culverts located at Meadow Rd., but did not inundate the roadway. The second event caused more intense flooding which overtopped the Meadow Rd. culverts for a longer time period. A portion of Meadow Rd. to the direct west of the culverts was inundated due to the inability of the culverts to discharge the flood waters. Simulation results using the modelled culvert scenario (current condition) were compared to in-situ observations on November 28th at 1230 (UTC) and show good agreement between modelled and observed water levels (Figure 3.1).

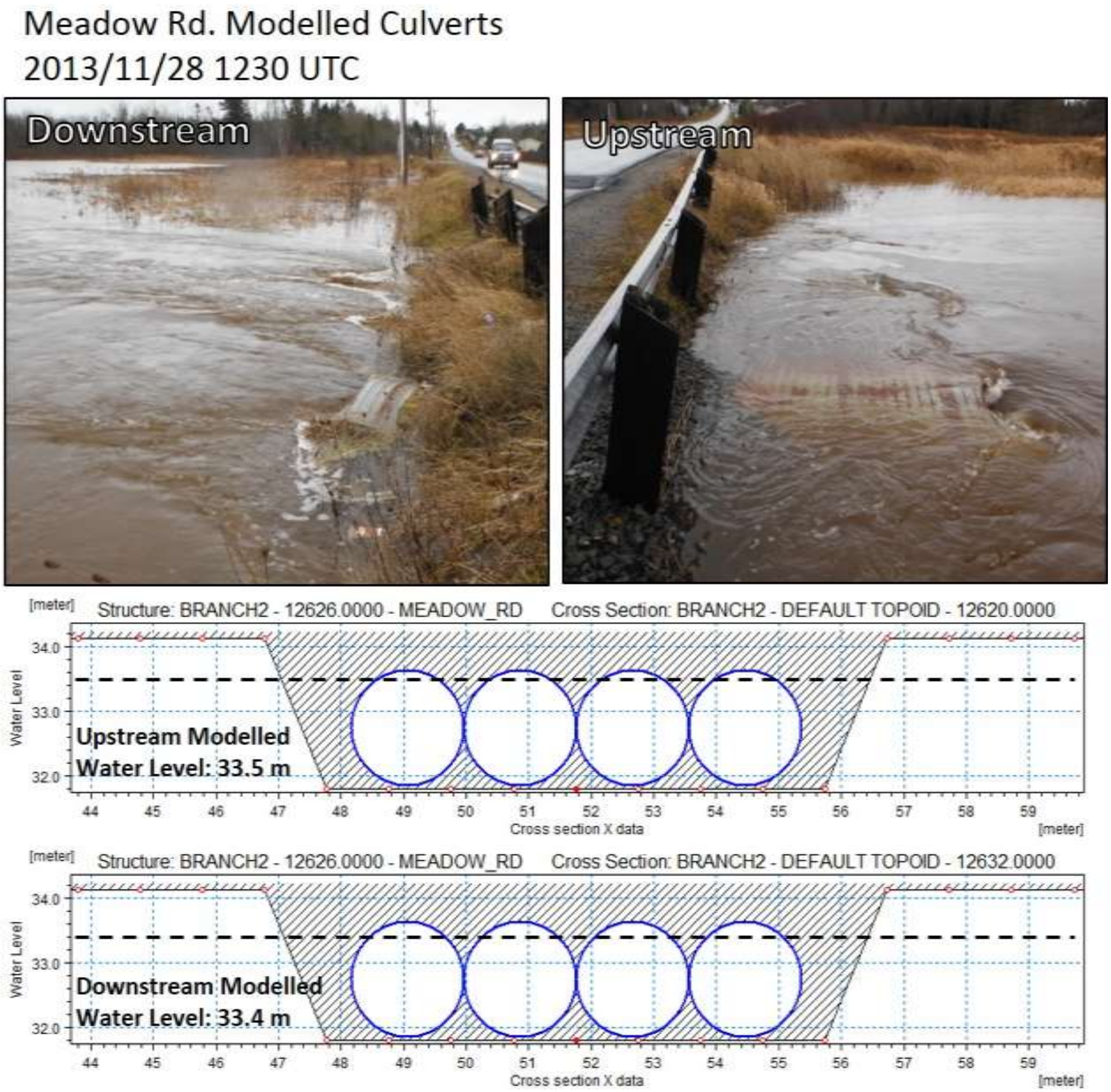

Figure 3.1: Model calibration results for the Nov 28, 2013 flood event at the Meadow Rd. culverts.

Model results were similarly compared at the Brown Flats Rd. culvert location where photos were taken at November 28th at 1245 (UTC);coincident simulation results showed good agreement between modelled and observed water levels (Figure 3.2).

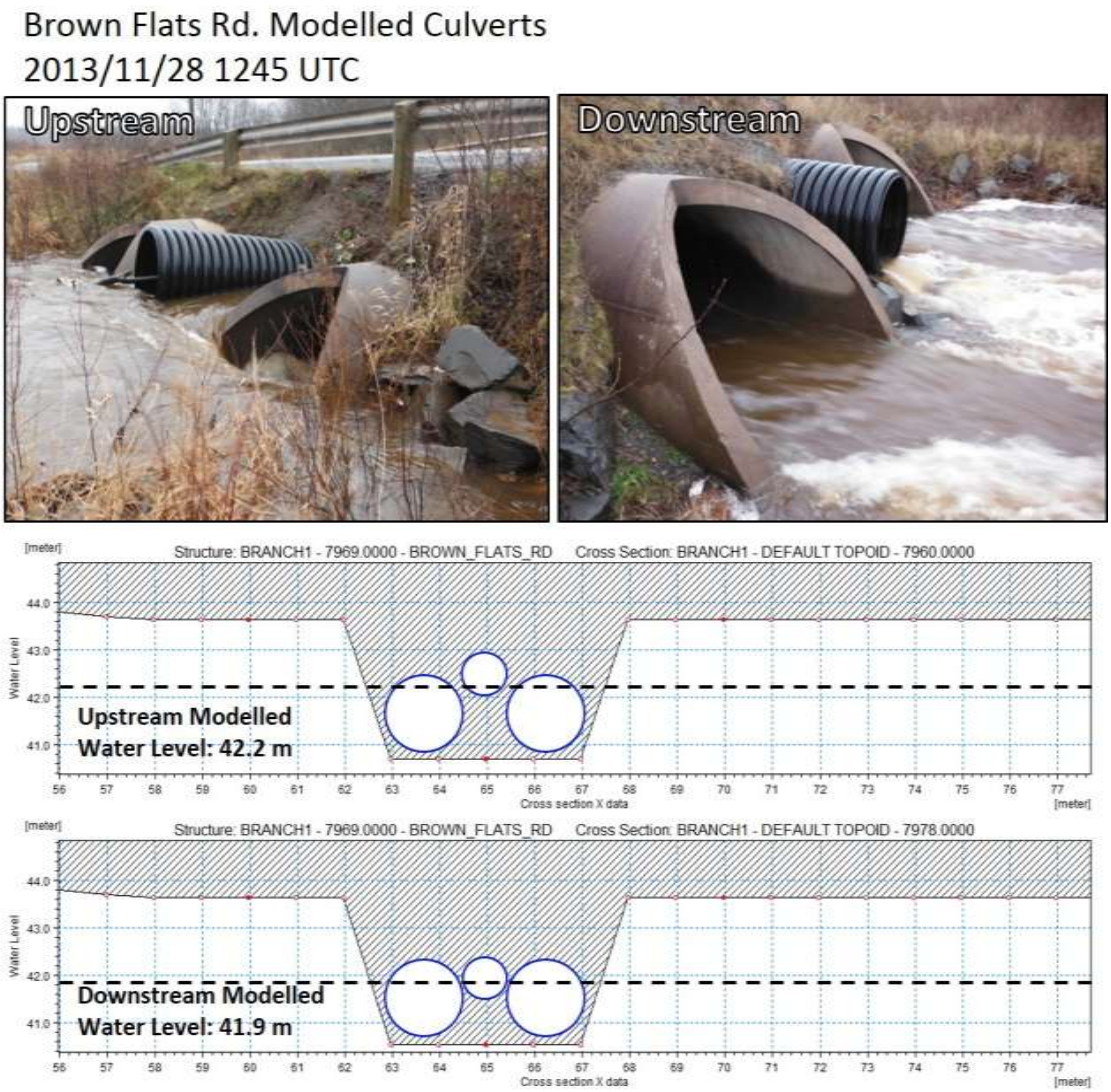

Figure 3.2: Model calibration results for the Nov 28, 2013 flood event at the Meadow Rd. culverts.

No overtopping of either Brown Flats Rd or Meadow Rd. occurred during the November 28th, 2013 event which agreed with the 2-D model peak flood results (Figure 3.3).

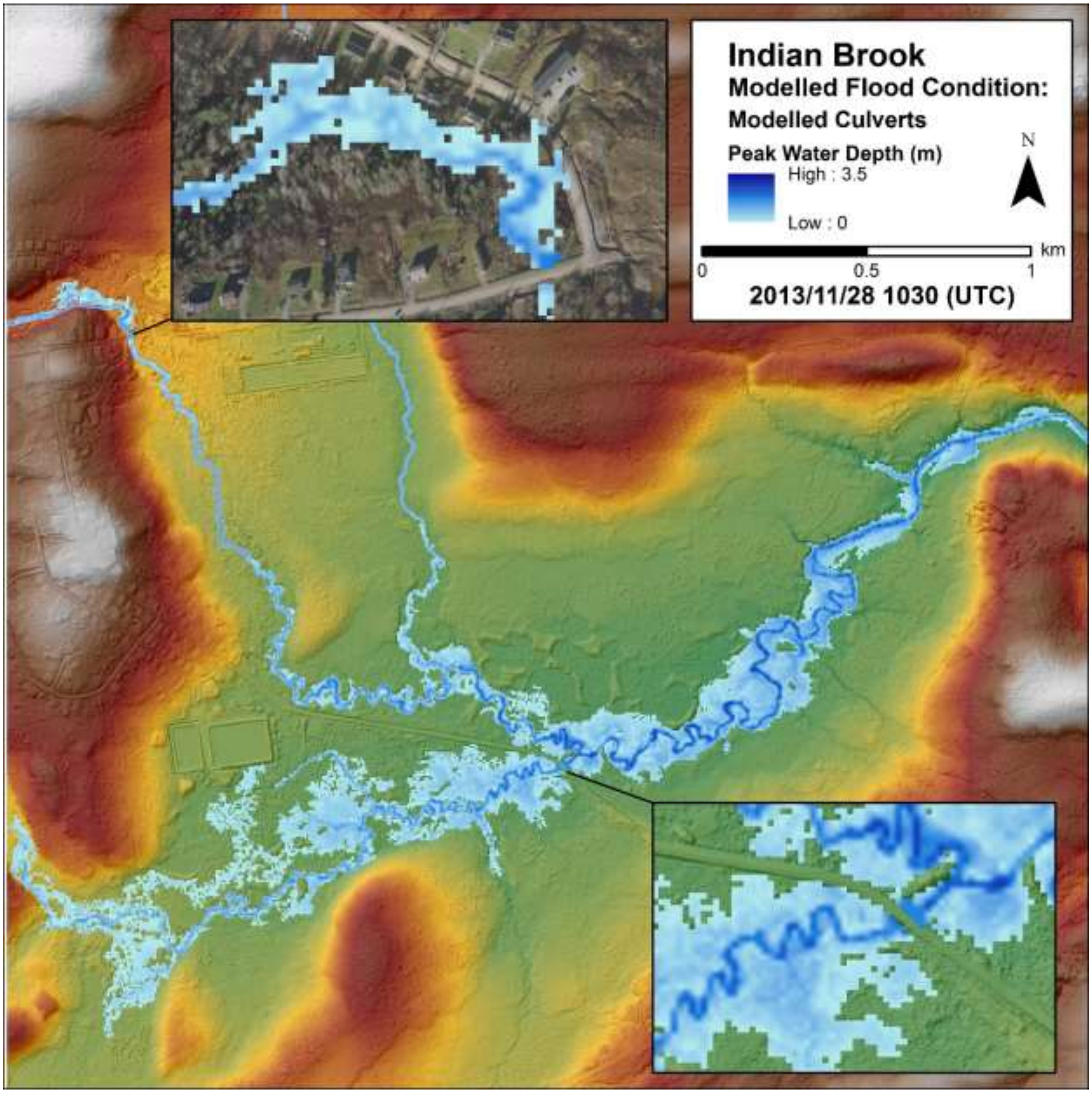

Figure 3.3: 2-D Model inundation map for the November 28th, 2013 flood event which shows no overtopping of Brown Flats Rd. (top inset) or Meadow Rd. (bottom inset) at the peak of flooding.

In-situ observations were used to validate model results for the higher intensity December 4th, 2013 flood event at the Meadow Rd. culvert location (Figure 3.4) and the Brown Flats Rd. culver location (Figure 3.5). Model results were again found to show good agreement between simulated and observed water levels at the culvert locations.

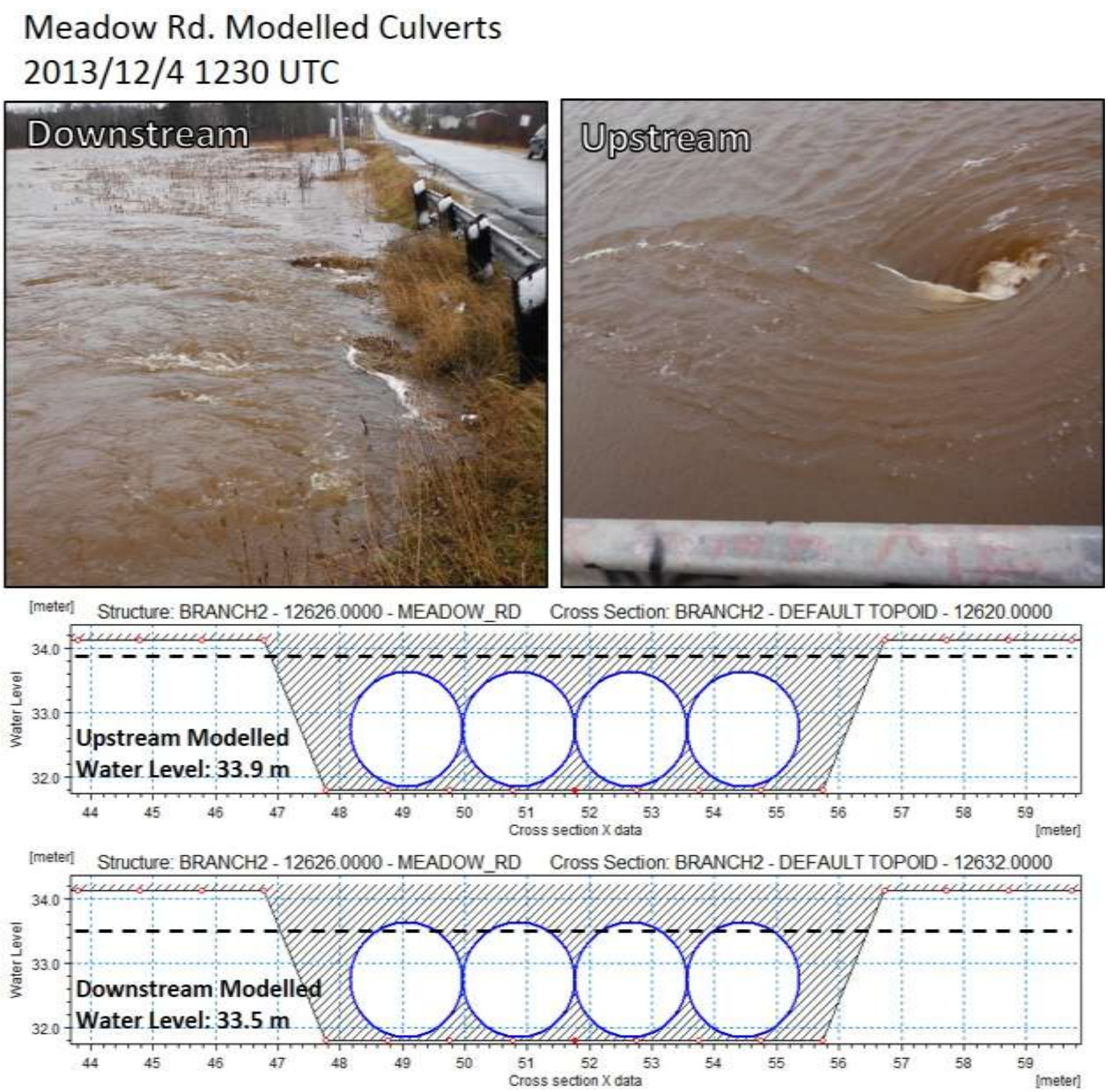

Figure 3.4: Model calibration results for the Dec 4, 2013 flood event at the Meadow Rd. with submerged culverts.

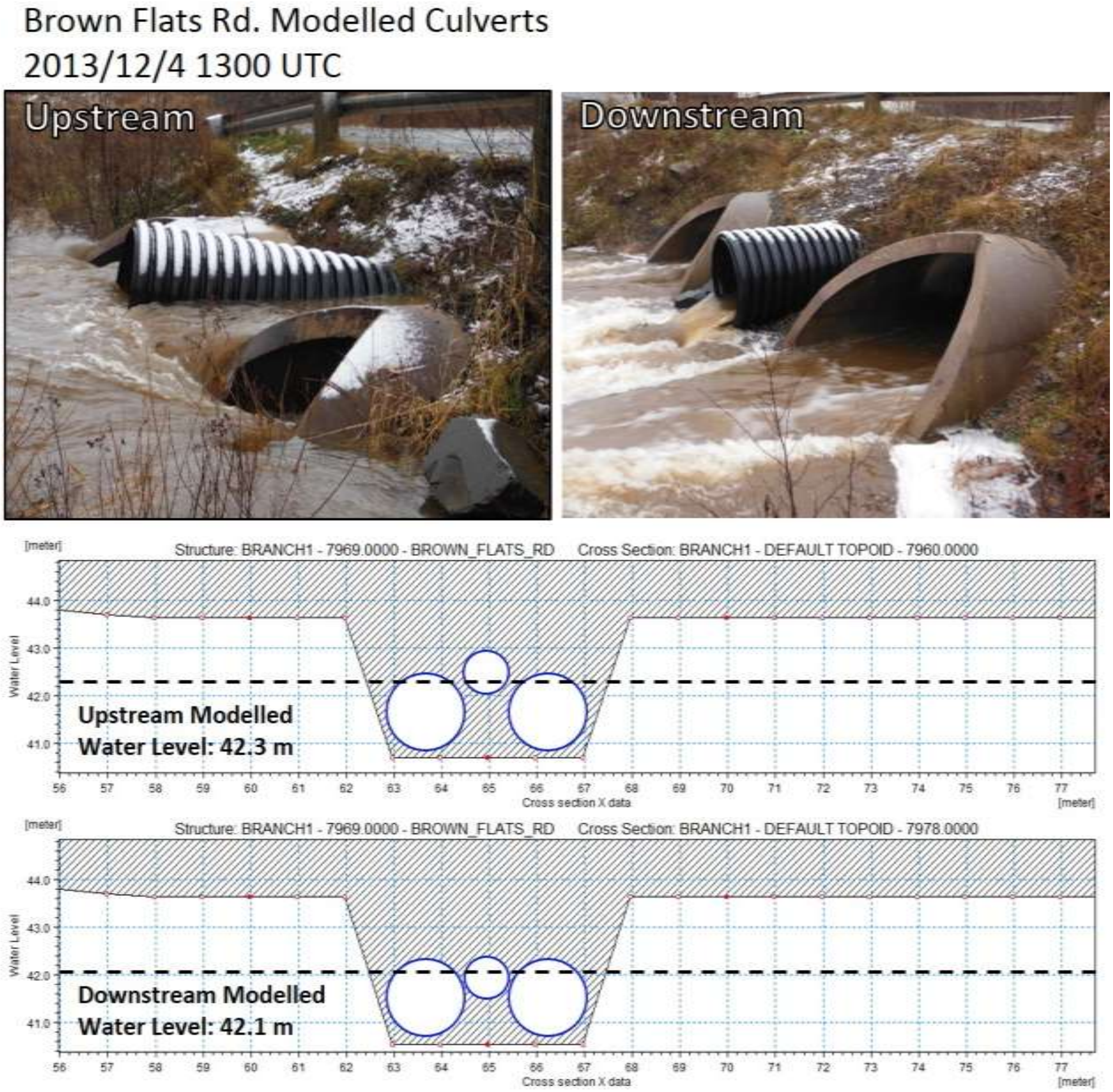

Figure 3.5: Model calibration results for the Dec 4, 2013 flood event at the Brown Flats Rd. culverts which show elevated water levels when compared to the Nov 28, 2013 flood event.

The 2-D hydrodynamic model calculated a 0.35 – 0.45 m inundation over Meadow Rd. at the peak flood period on December 4, 2013 at 1230 UTC (Figure 3.6). This result agreed with in-situ observations and photographs of the flood event (Figure 3.7). In both the model results and in-situ observations, the roadway remained partially inundated for several hours with flood waters receding 5 hours after the peak of flooding.

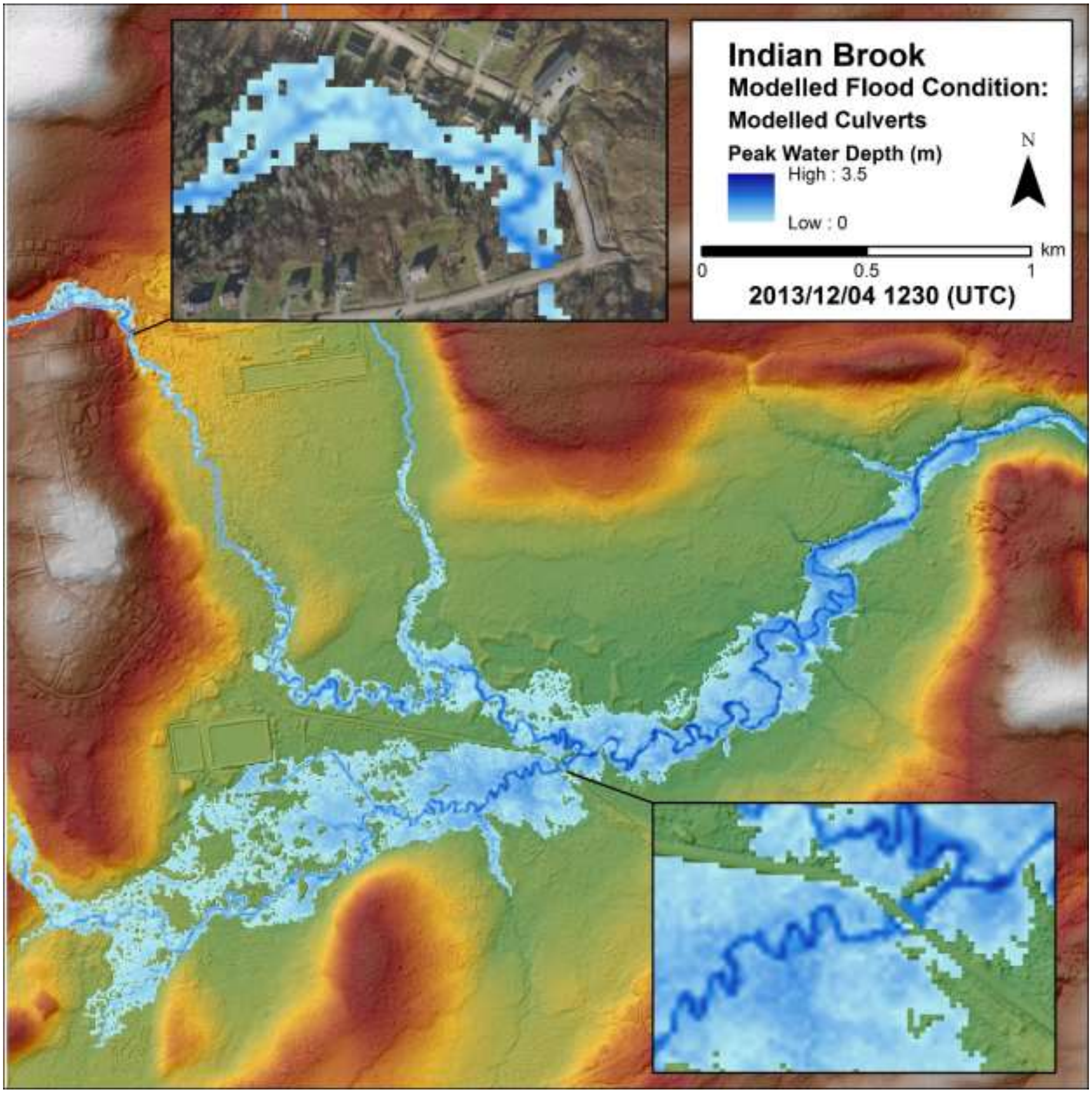

Figure 3.6: 2-D Hydrodynamic model results show inundation occurring at the peak flood period over a portion of Meadow Rd. (bottom inset) to the northwest of the culvert locations.

Figure 3.7: Photograph of inundation over Meadow Rd. directly northwest of the culvert location taken December 4th, 2013 at 1230 UTC.

The 2-D and 1-D hydrodynamic models were determined to be valid based on the level of agreement between model results and in-situ observations.

3.2 Model Simulation Results

With the models validated, it was possible to run simulated scenarios in which model variables could be adjusted to account for: the replacement or refinement of engineered structures, modified environmental conditions, and modified topography, as described in Section 2.3and presented in Table 2.3.

3.2.1 Modelled Culverts

Modelled culverts were found produce realistic results compared to in-situ observation. The Meadow Rd. culverts discharged a maximum of 33.81 m^3/s at their peak. This discharge rate was insufficient to route volume of precipitation and the culvert became overtopped (Figure 3.8). Flood waters reached a maximum elevation of 33.9 m upstream of the culverts. The level of water was sufficient to flood a portion of Meadow Rd. as discussed in the above validation section.

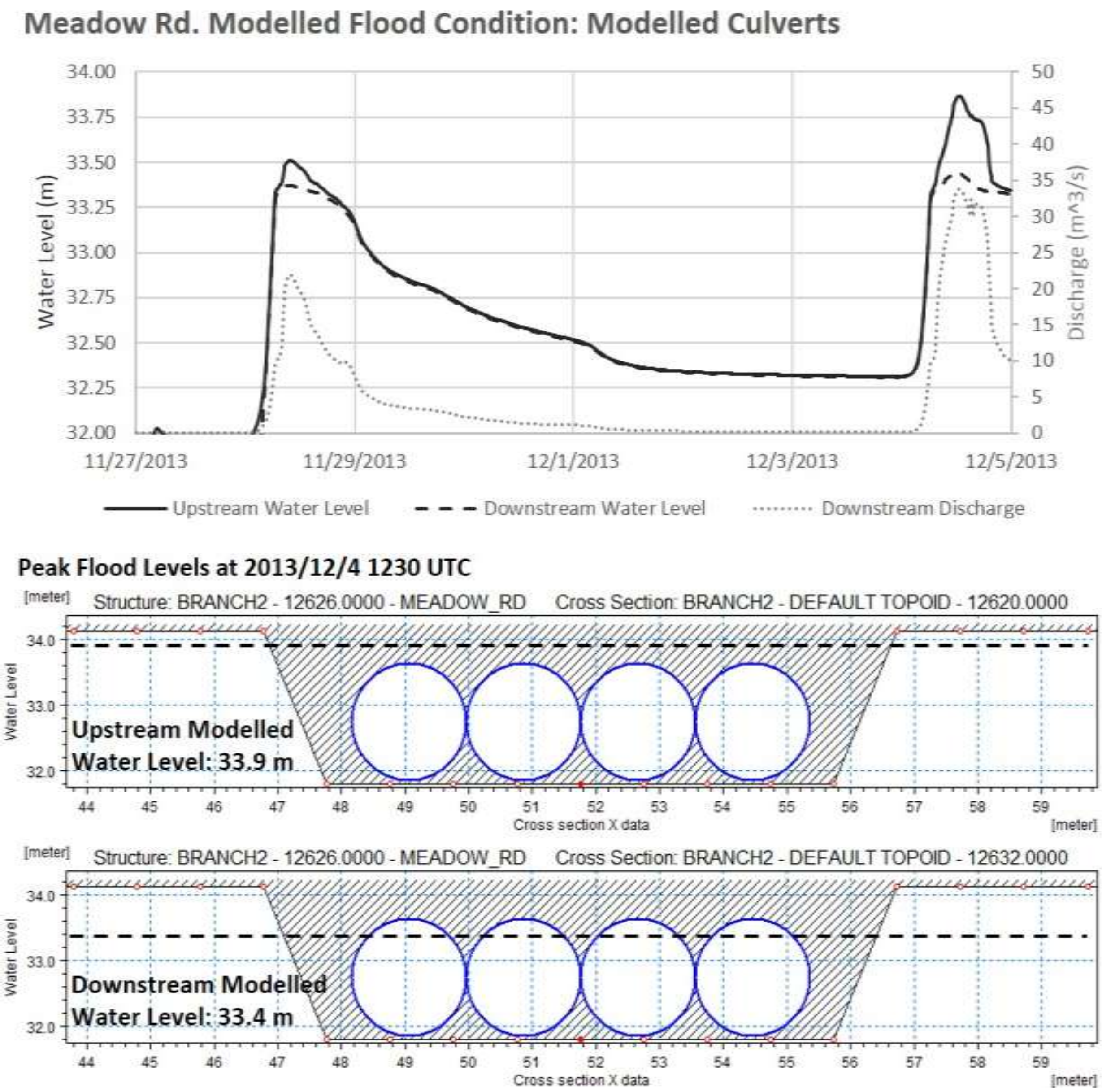

Figure 3.8: Simulation results for the Meadow Rd. study area using modelled culverts which represent current conditions.

Contrarily, the culverts at Brown Flats Rd. were able to successfully handle the volume of rainfall without becoming submerged and discharged a maximum of 15.34 m^3/s during the peak of the flood event. Flood waters reached a maximum elevation of 42.4 m upstream of the culverts (Figure 3.9).

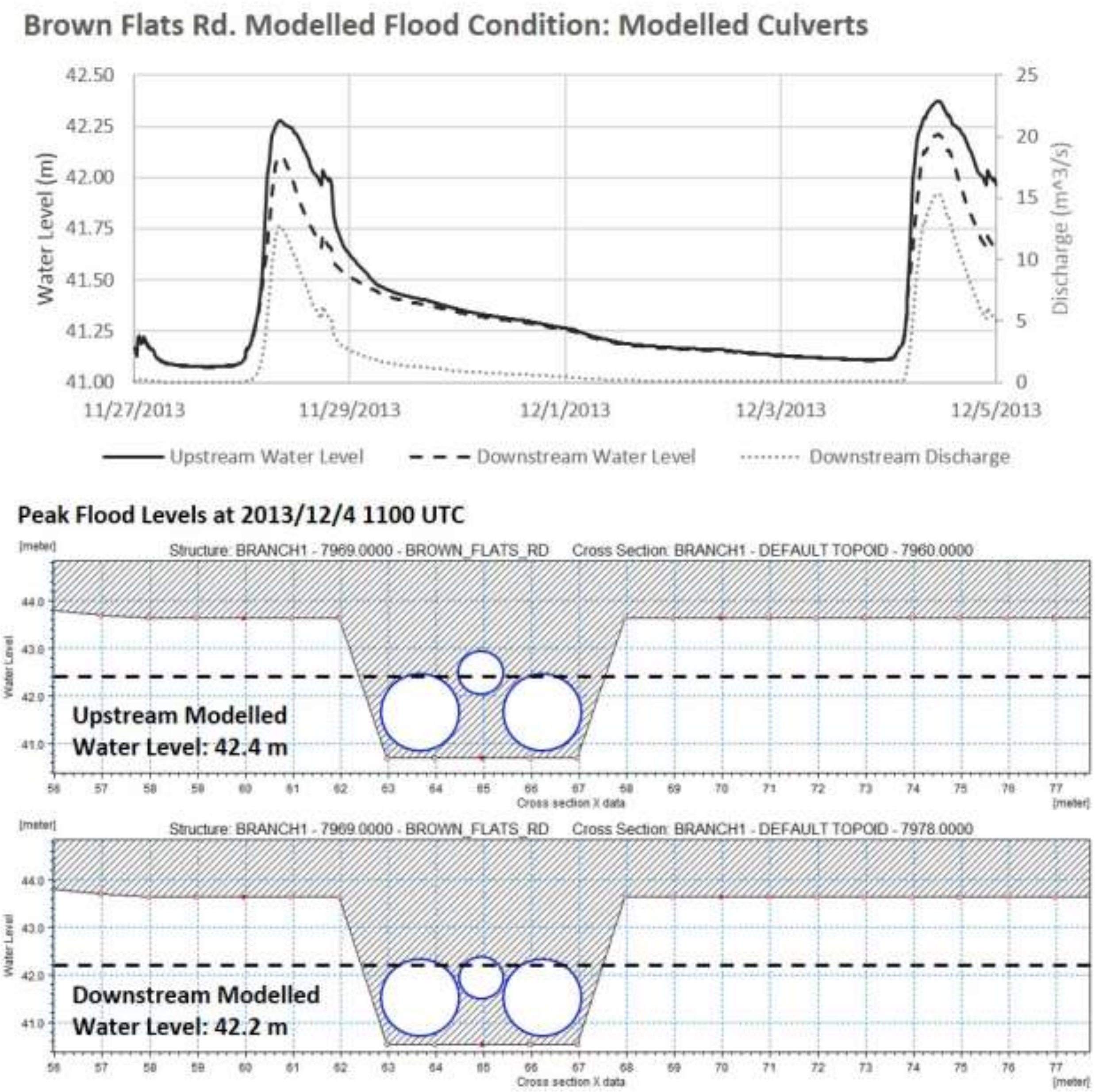

Figure 3.9: Simulation results for the Brown Flats Rd. study area using modelled culverts which represent current conditions.

3.2.2 Cleared Culverts

The cleared culverts condition successfully routed runoff more effectively than modelled culverts in the Meadow Rd. location. The culverts reached a maximum discharge rate of 32.49 m^3/s over the simulation period. Flood waters reached a maximum elevation of 33.7 m upstream of the culverts (Figure 3.10).

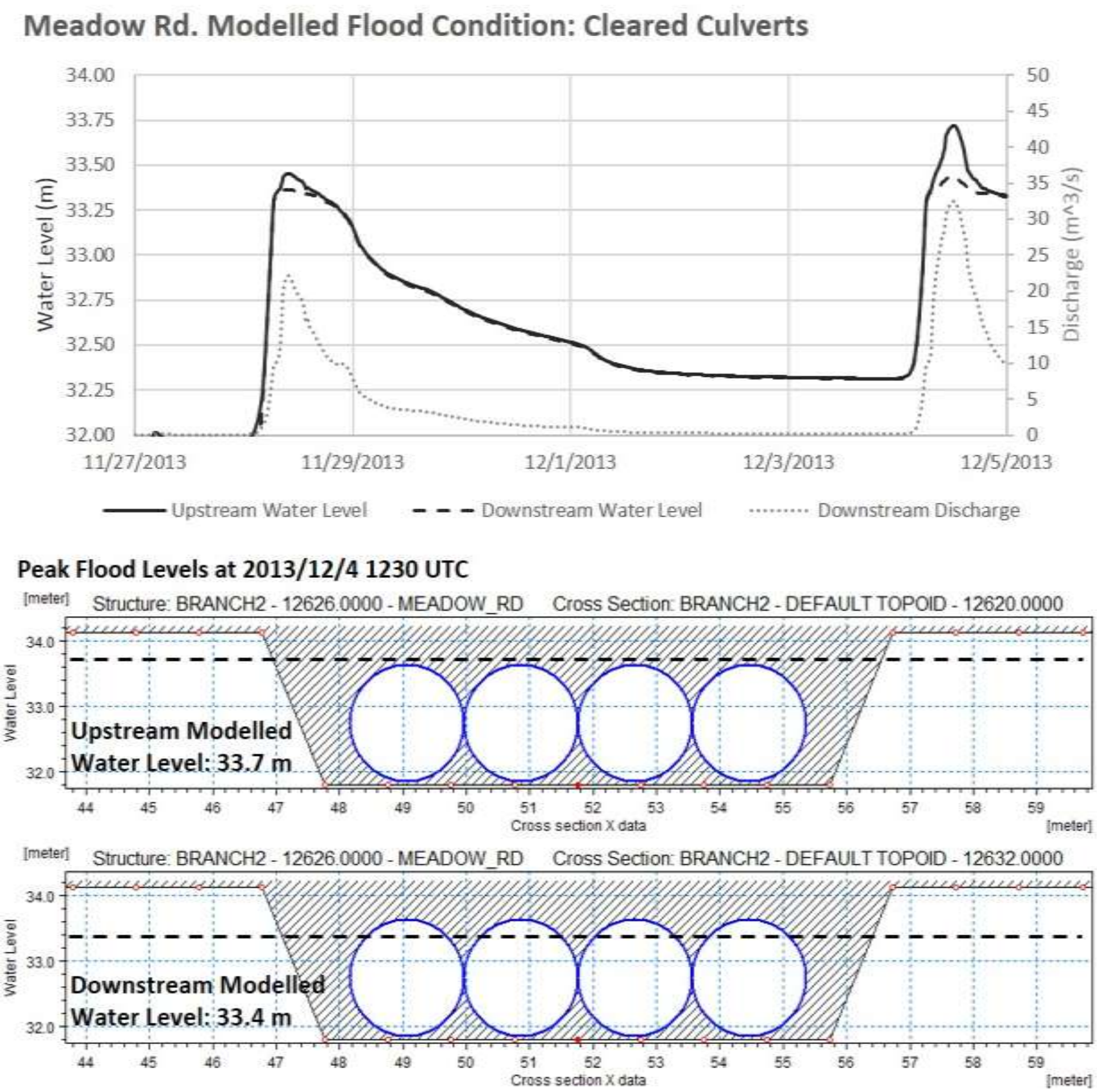

Figure 3.10: Simulation results for the Meadow Rd. study area using cleared culverts which reduced the duration and elevation inundation.

The increased efficiency of the culverts reduced the inundation depth over Meadow Rd. to 0.24 m during the flood event (Figure 3.11). Results are not presented for the Brown Flats Rd. culverts because they were reported to be cleared and are identical to the modelled culvert scenario.

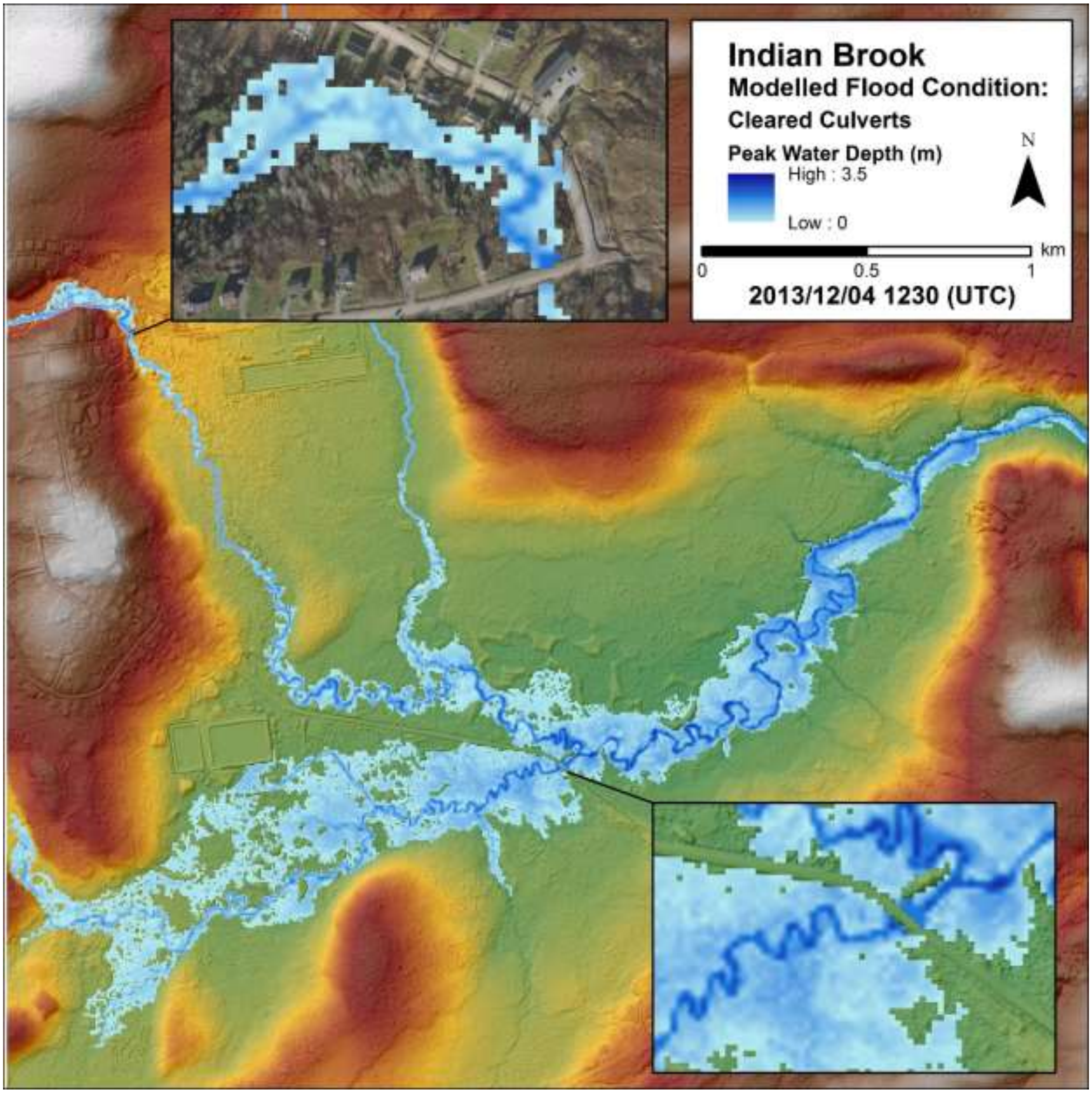

Figure 3.11: 2-D Hydrodynamic model peak flood extents for the Nov 28th to Dec 5th 2013 flood event that show a reduced flood extent and traversable Meadow Rd. (bottom inset) when culverts have been cleared.

3.2.3 Impeded Culverts

The impeded culverts condition successfully reduced the effectiveness of culverts to route water over the simulation period. Culverts at Meadow Rd. reached a maximum discharge rate of 31.29 m^3/s and were overtopped during the simulation by flood waters that reached a maximum elevation of 33.9 m upstream of the culverts (Figure 3.12). Culverts at the Brown Flats location achieved a maximum discharge rate of 8.16 m^3/s resulting in a maximum flood water elevation of 42.4 m upstream of the culverts (Figure 3.13).

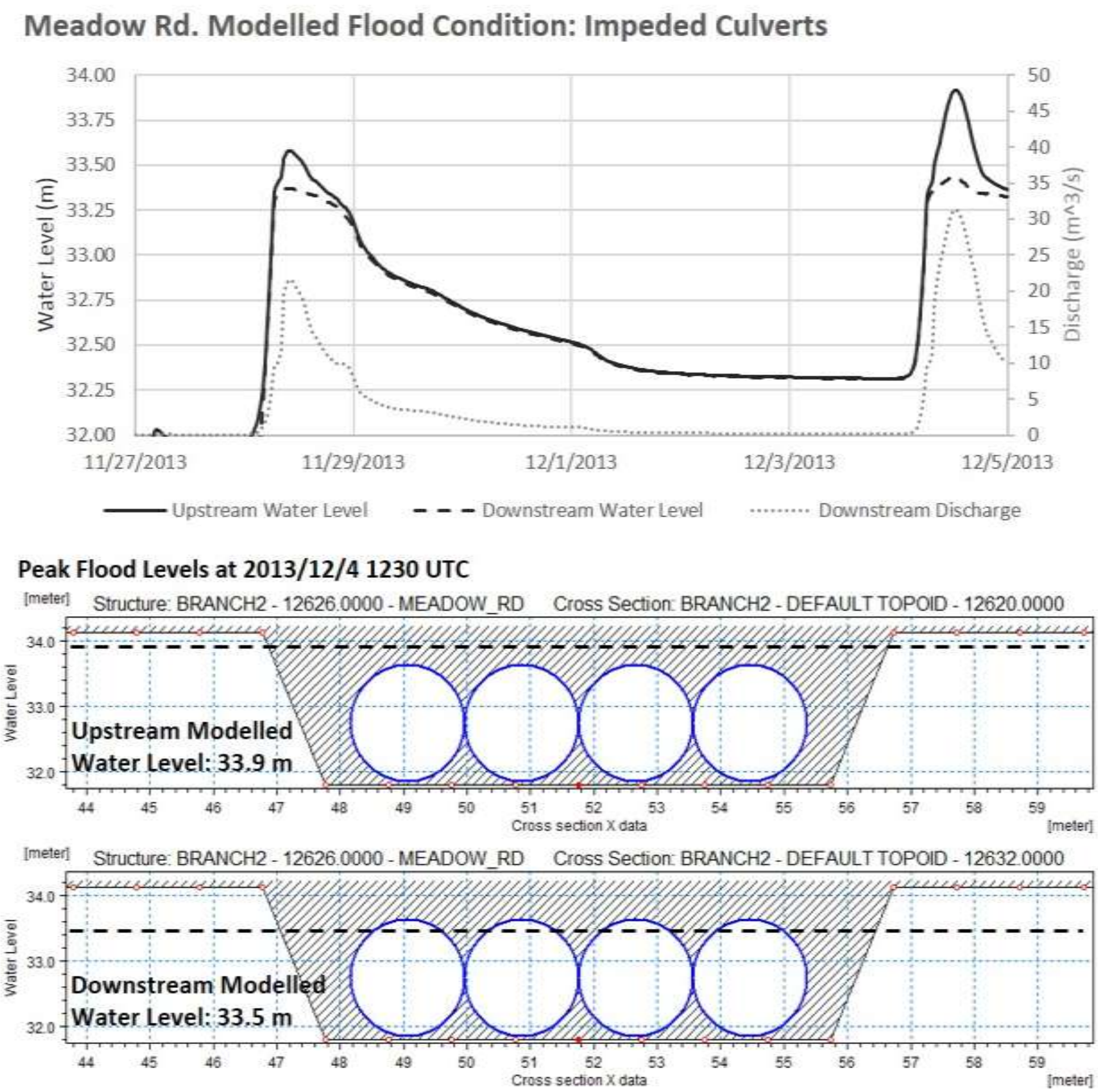

Figure 3.12: Simulation results for the Meadow Rd. study area using the impeded culverts condition which increased the duration of inundation.

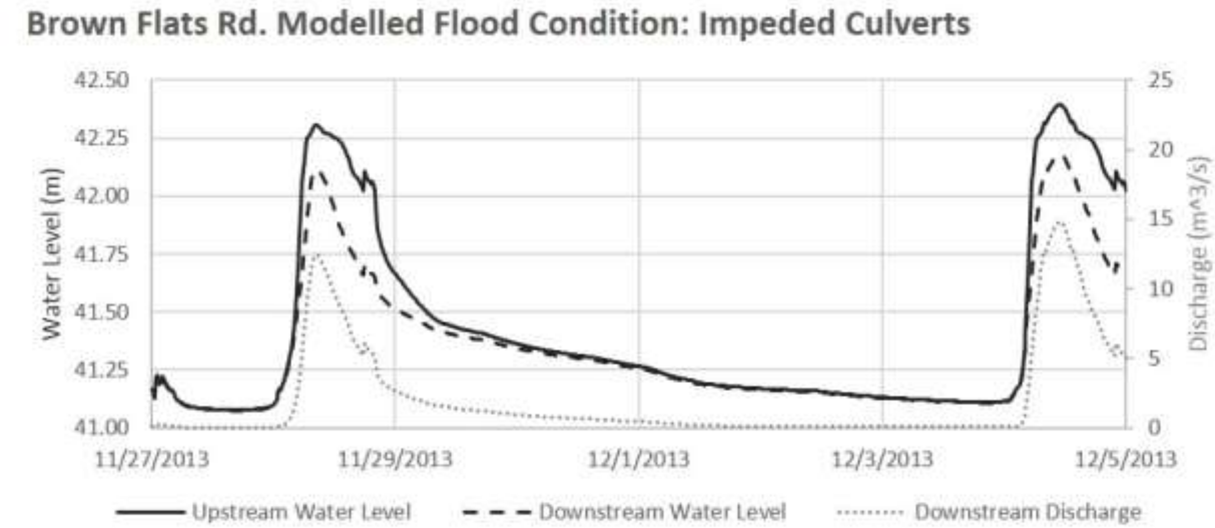

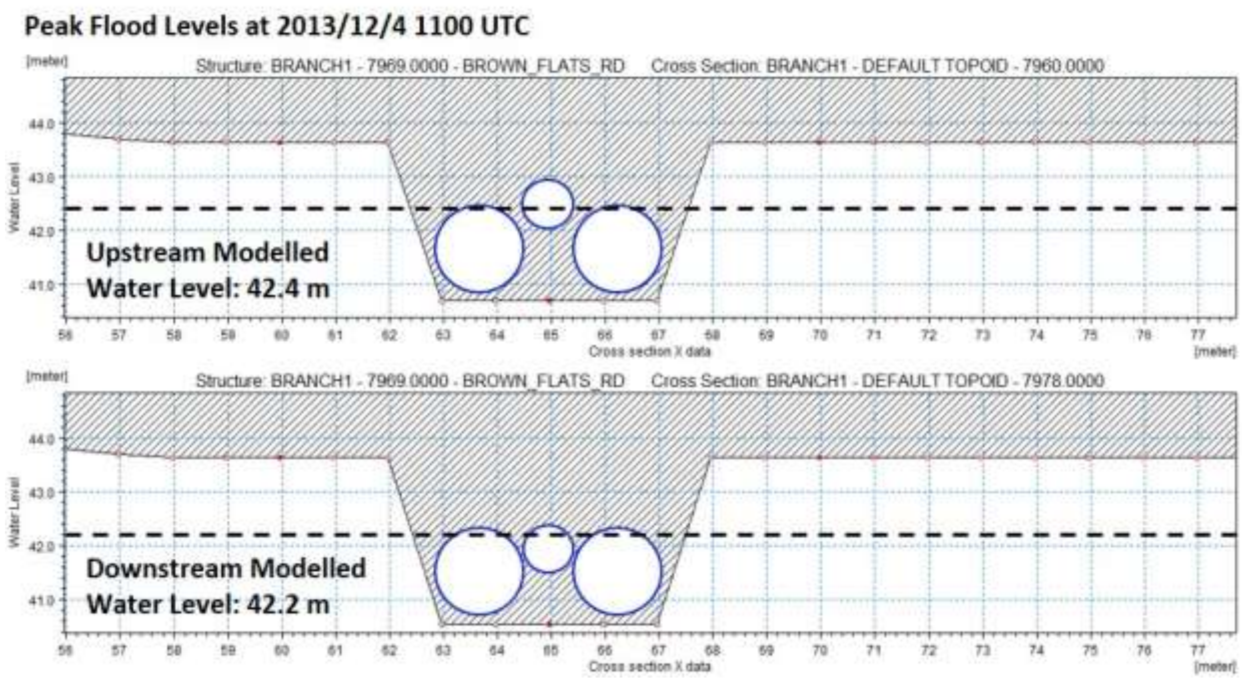

Figure 3.13: Simulation results for the Brown Flats Rd. study area using the impeded culverts condition which increased the time necessary to route the flood waters.

The impeded culverts lead to increased inundation depths and extents in areas upstream of the culverts. Meadow Rd. was overtopped at a depth of 0.42 – 0.52 m (Figure 3.14).

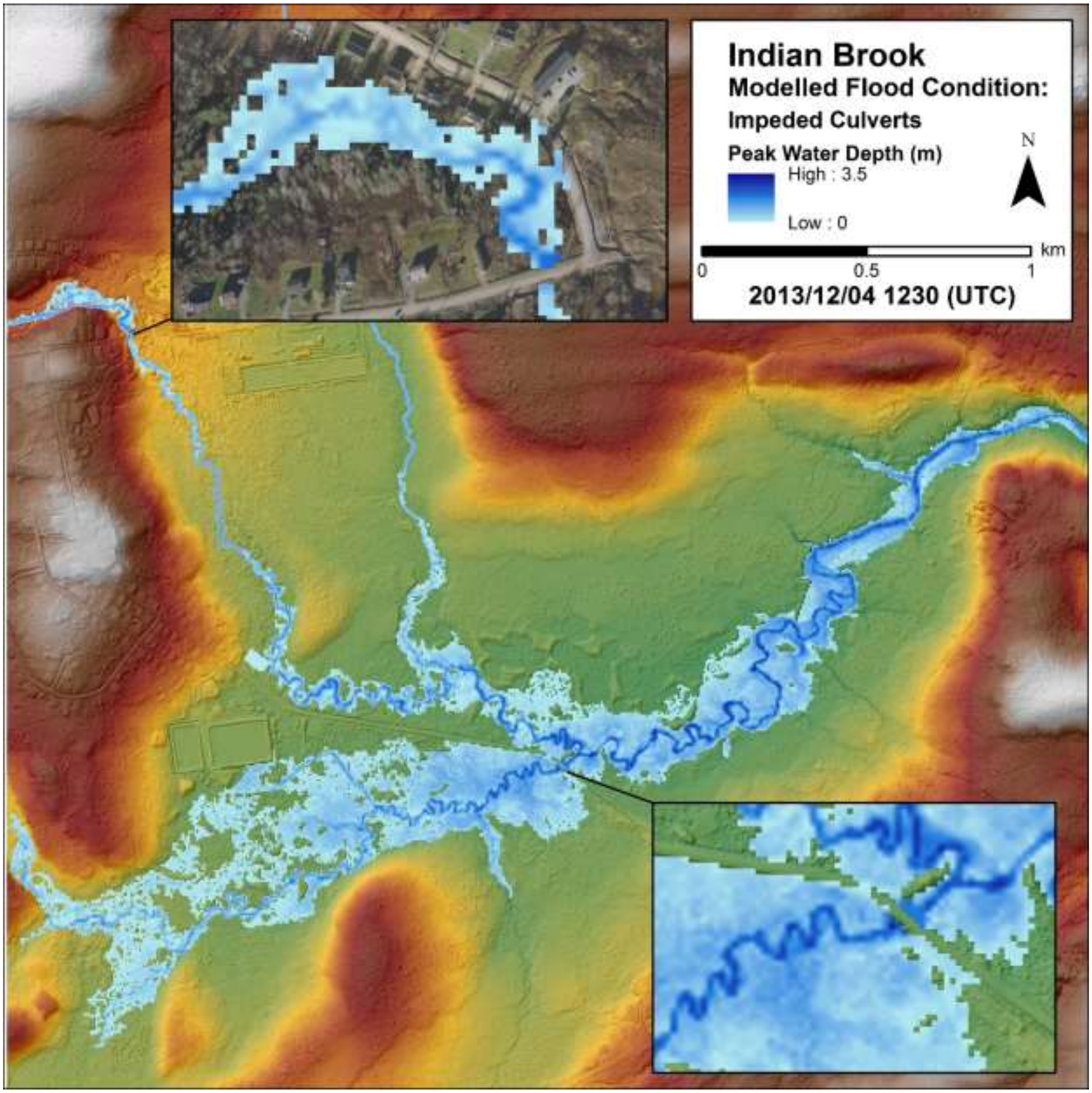

Figure 3.14: 2-D Hydrodynamic model peak flood extents for the Nov 28th to Dec 5th 2013 flood event that show an increased flood extent and inundated Meadow Rd. (bottom inset) when culverts have been impeded.

3.2.4 Culverts Replaced with Bridges

Culvert beds were replaced with open flow bridges which dramatically increased the ability of the bottlenecks to route floodwaters. A bridge was added at the Meadow Rd. location (9 m wide, 2.5 m deep) that discharged a maximum of 33.12 m^3/s during the simulation period and reduced the maximum flood water elevation to 33.5 m upstream of the bridge (Figure 3.15). The bridge added at the Brown Flats Rd. location measured 5 m wide by 3 m deep and discharged a maximum of 14.46 m^3/s. Flood levels upstream of the bridge reached a maximum elevation of 42.4 m (Figure 3.16).

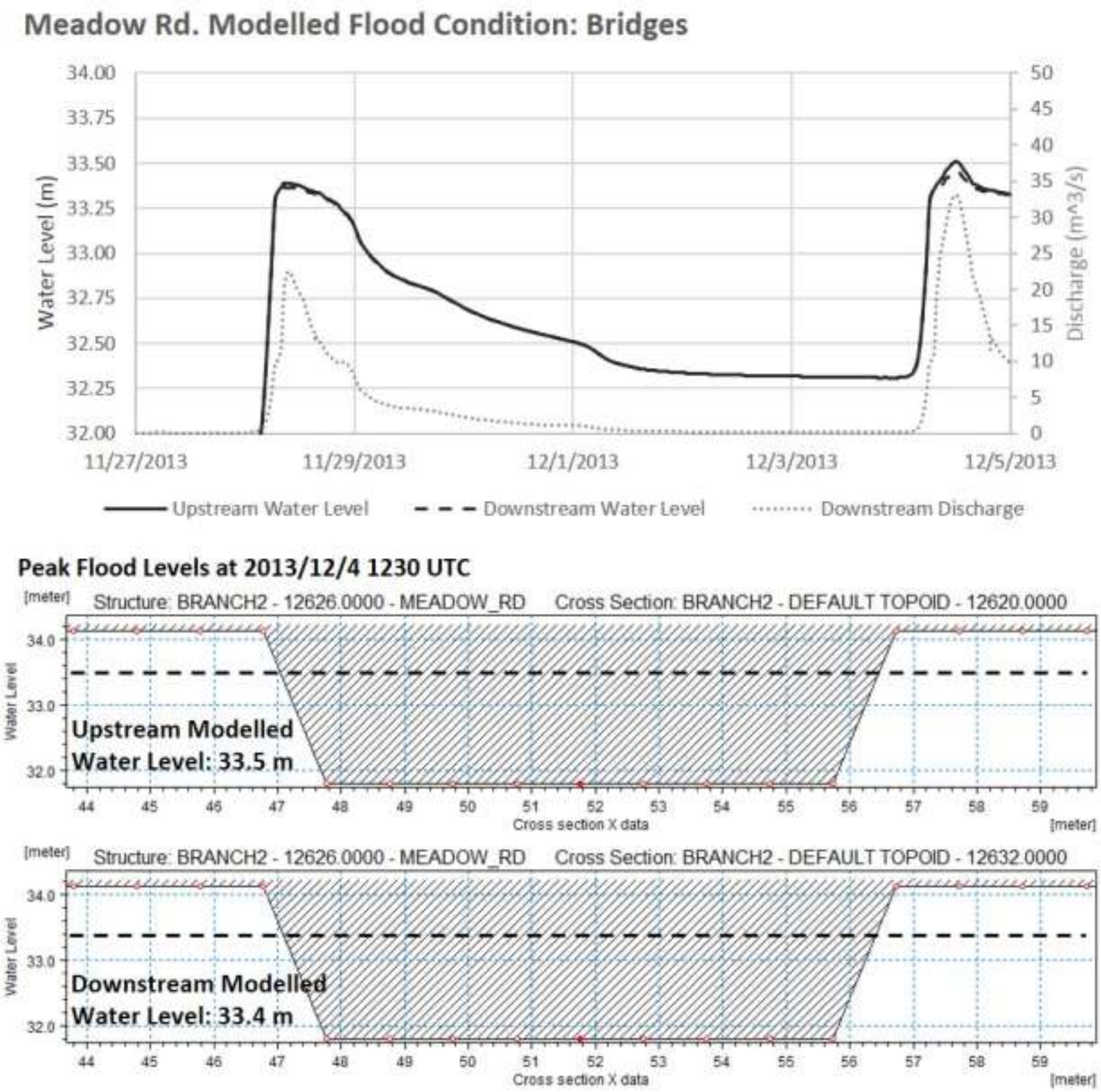

Figure 3.15: Simulation results for the Meadow Rd. study area with culverts replaced by bridges which dramatically reduced the time required to route flood waters.

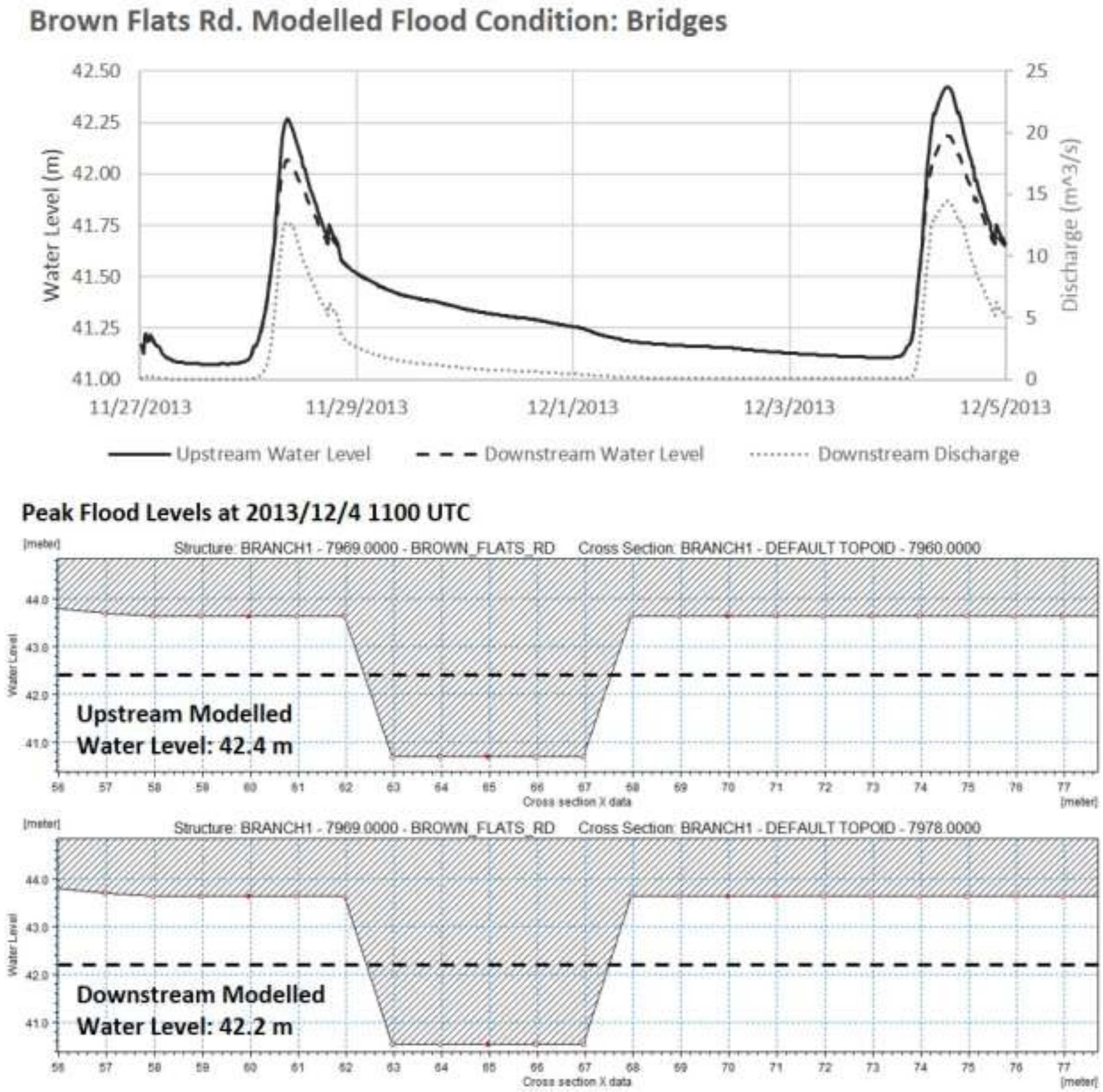

Figure 3.16: Simulation results for the Brown Flats Rd. study area with culverts replaced by bridges which effectively routed flood waters.

The bridges reduced the extent and severity of flooding in areas upstream of the bridges and prevented inundation of Meadow Rd. (Figure 3.17).

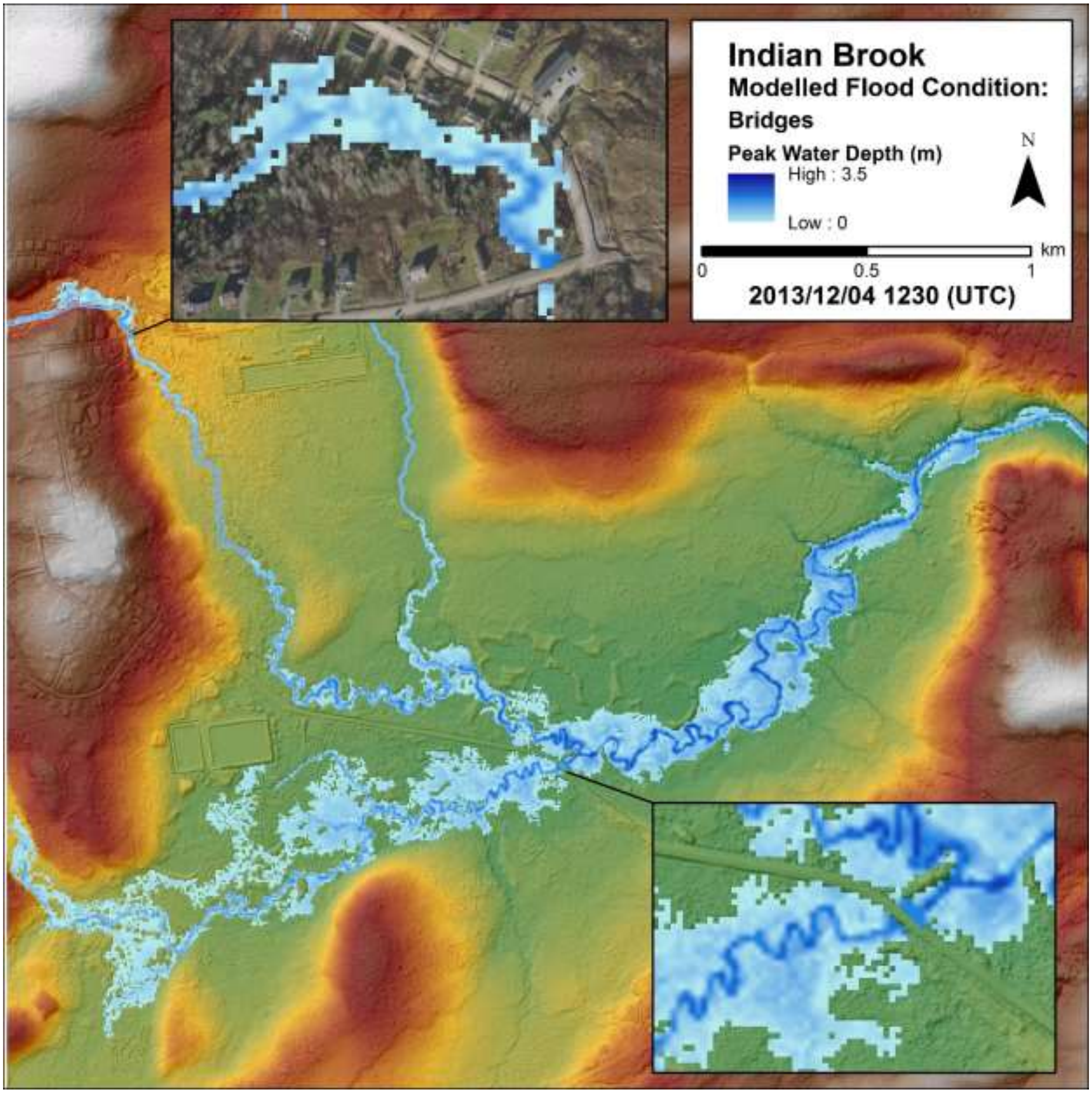

Figure 3.17: 2-D Hydrodynamic model peak flood extents were reduced and Meadow Rd. (bottom inset) remained traversable by replacing culverts with bridges for the Nov 28th to Dec 5th 2013 event.

3.2.5 Increased Precipitation Intensity

The model inputs were adjusted to increase the intensity of precipitation events by 16% in accordance with the climate change projections of Richards and Daigle (2012). The increase in rainfall intensity effectively increased the volume of flood water entering the total watershed area (48.09 km^2) from 6.72 $x10^6$ m^3 to 7.80 x 10^6 m^3 over the simulation period from November 27th to December 5th, 2013. The volume of water in the watershed upstream of the Meadow Rd. culverts (19.78 km^2) increased from 2.77 x 10^6 m^3 to 3.21 x 10^6 m^3 over the event. Flooding caused by the increased rainfall was simulated using the modelled culvert condition. The modeled culverts achieved a maximum discharge rate of 33.5 m^3/s when overtopped. A peak water elevation of 33.9 m was recorded directly upstream of the culverts but extensive flooding was observed in the 2-D model which calculated the inundation of Meadow Rd. at a depth of 0.5 – 0.6 m for a period lasting 6 hours (Figure 3.18).

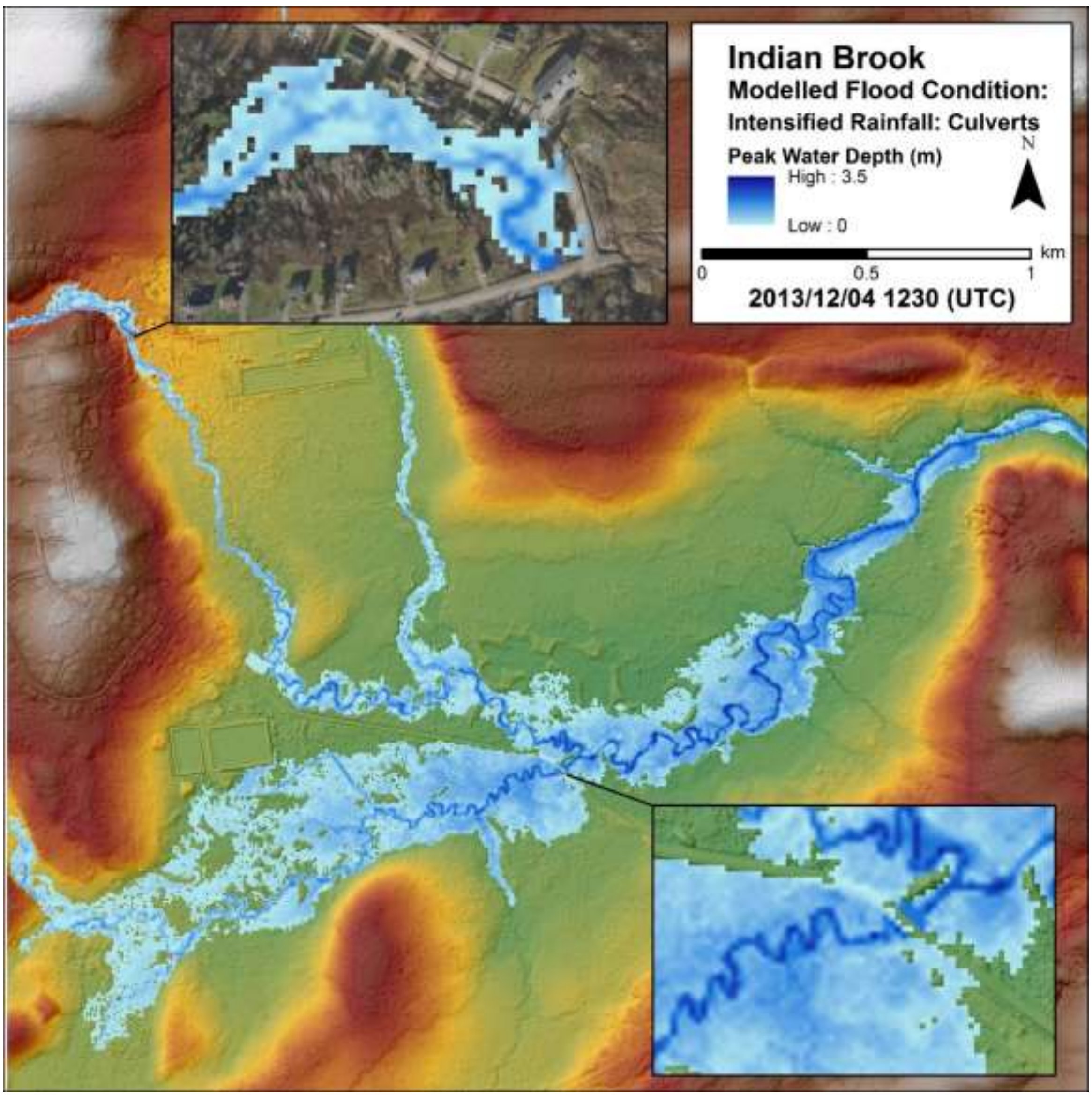

Figure 3.18: Hydrodynamic model peak flood extents were significantly increased in response to climate change and flood magnitude was sufficient to submerge Meadow Rd. (bottom inset) west of the culvert locations at a depth of 0.5 – 0.6 m

Flooding due to intensified rainfall was also modeled using the bridge replacement condition. Model results showed less intense overall flooding and the preservation of the Meadow Rd. section prone to inundation (Figure 3.19).

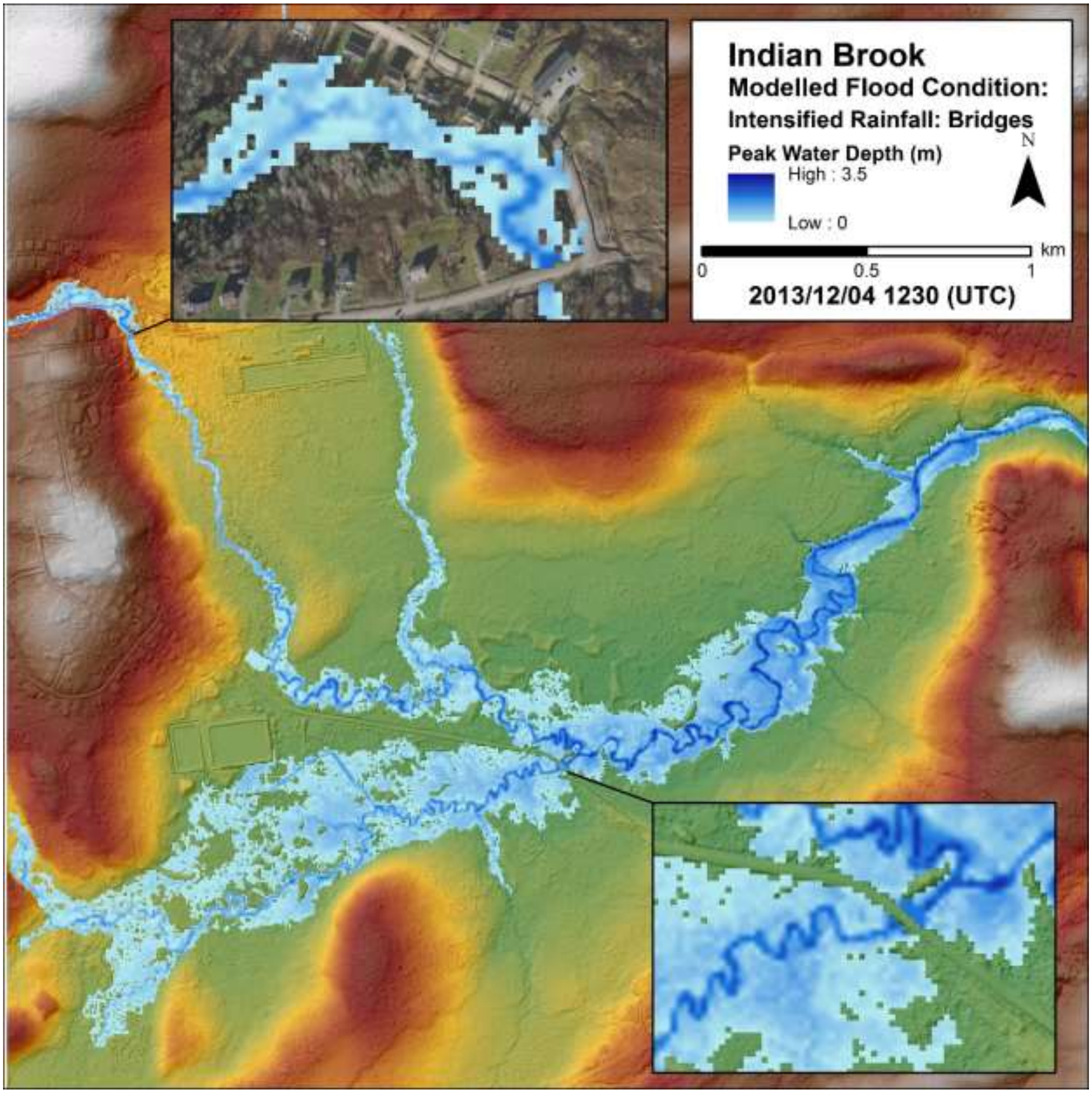

Figure 3.19: Hydrodynamic model peak flood extent in response to climate change projections for increased precipitation over the Nov 28th to Dec 5th 2013 event for the bridge replacement condition. Flood levels were not sufficient to inundate Meadow Rd. (bottom inset).

4 Discussion and Conclusions

The developed hydrodynamic models were found to realistically simulate inundation levels and extents using measured environmental variables (precipitation), culvert measurements, and a terrain model of the Indian Brook study area as model inputs. The validated models were used to generate comparative condition based models which impacted the inundation characteristics of the flood event for the period of November 27th to December 4th, 2013 (Table 4.1).

Condition	Meadow Rd. Flood Levels: Water Level Upstream of Culverts (m)	Meadow Rd. Flood Levels: Floodwater Depth Over Roadway (m)
Modelled Culverts	33.87	0.36
Impeded Culverts	33.92	0.42
Clear Culverts	33.72	0.24
Bridges	33.51	0.00
Intensified Rainfall: Modelled Culverts	33.91	0.50
Intensified Rainfall: Bridges	33.73	0.10

Table 4.1: Inundation levels over the Meadow Rd. infrastructure in response to modelled structural and environmental conditions.

Model results show a clear potential threat to human safety and infrastructure during significant rainfall events. The main bottleneck of the drainage system is located at the Meadow Rd. culvert bed. These culverts are responsible for draining nearly 20 km^2 of watershed area. The topography in the area upstream of the bottleneck is a shallow floodplain that quickly becomes flooded in the event that the culverts cannot route the incoming flood waters. Inundation caused by the bottleneck threatens a nearby sewage treatment plant and the Meadow Rd. infrastructure. Comparisons between model condition results show that the existing culverts at the Meadow Rd. location are unable to route the water from prolonged rain events whether in new condition (cleared culverts), current condition (modelled culverts) or deteriorating condition (impeded culverts). The bottleneck was found to perform much more efficiently when the culverts were replaced with a bridge structure and flood waters were successfully routed with minimized flooding in this condition. The bridge condition performed particularly well even in climate change scenarios where the intensity of rainfall was increased by 16% resulting in an additional 0.448×10^6 m^3 of water landing upstream of the bottleneck. Despite the increase in load, the bridge condition was found to minimize flood extents and depths to levels below the non-intensified rainfall condition with cleared culverts. No flood conditions were found to overtop the roadway by more than a meter during the simulated events. This result suggests that raising the road will potentially protect it from inundation. Raising the roadway will effectively increase the amount of time required to overtop the infrastructure once the culverts are unable to route incoming water but will not prevent a threat in prolonged events. Any plans to raise the roadway should also take into consideration the sewage treatment plant located upstream which is protected by a berm only 2 m higher than the existing Meadow Rd. surface.

The failure to simulate flooding over Brown Flats Road is a limitation of the model given the frequency of flood events there and the risk they pose to community members isolated and put at risk by such events. A likely explanation is that the laser data used to build the elevation model did not penetrate the forest canopy sufficiently during the lidar survey, resulting in a DEM that is higher than in reality. Since the lidar elevation data in this area does not accurately represent the topography, the runoff is confined to the stream and flows through the three-culvert system (Culvert 2A,B,C, Figure 2.5) rather than spilling over, running through the wooded area and overtopping the road near Culvert 2-D,E,F,G as we know it does (Figure 1.6c,d). The solution to this problem is to return to Indian Book and survey the road and area near Culvert 2 using RTK GPS, adjust the DEM, and re-run the model.

Flood events reported at Tower Road and Robinson Road were not captured by the current model because the areas fall outside the high resolution terrain model domain. Floodplains in these areas cannot be mapped due to the lack of adequate terrain data. If the primary concern in these areas is not the extent of upstream flooding, but the depth of water over roadways and structures, water levels can be captured within the 1-D hydrodynamic model if additional data are collected using an RTK GPS to establish cross-sections at these bottlenecks.

The November and December 2014 floods (Figure 2.6 and Figure 2.7) were major rainfall and high water events. Unfortunately, at the time of this report, we do not have pressure sensor data during these flood events to validate the model. Once the stage sensor is retrieved, those flood events can be modelled and compared to observations. It is possible to run the model without observed water level to validate against, and instead compare results to photographic evidence of road overtoppings and measured culvert heights; if the water level data are poor quality or if there was a sensor failure, this will be the course of action.

5 Future Work

A final phase of hydrodynamic model refinement will occur in Phase III. This will involve collecting additional RTK GPS data including the area near Brown Flats Road so that flood events there may be better modelled. Climate change and infrastructure adaptation simulations can then be accomplished. Additionally, the water level sensor at Bridge 2 will be recovered once the river ice melts. This will allow us to test the model performance during the flood events of November and December 2014 against the observed water level data.

Moving into Phase III we will work with MAPS to embed the hydrodynamic model into the community's infrastructure maintenance and development planning processes. This will involve using the adaptation simulation results as a basis for the community's interaction with a hydrological engineering firm. We will also work with MAPS to incorporate the flood risk model into the local emergency response protocol; this will involve a quantification of the relationship between rainfall and flooding, so that officials can adequately prepare for potential flooding using a forecasted heavy rainfall event.

The hydrodynamic model will be used as the basis for a contamination disbursement plan in Phase III. Drinking water supplies have been contaminated at Indian Brook in the past, necessitating a water management plan. To accomplish this, we will survey subsurface infrastructure in the Indian Brook Watershed, examine and map sources of fecal coliform, and develop a contamination disbursement model to be linked with the Mike 1-D/2-D hydrodynamic model. The model will be used to develop a water management plan for the community and reduce contamination of drinking water sources.

The completion of the incorporation of traditional knowledge, model results and spatial data including lidar and orthophoto products into a geodatabase will occur in Phase III, and we will present and summarize all the deliverables from Phases I, II and III at a final community meeting.

6 References

APTN National News (2012). Indian Brook awash in flood waters. http://aptn.ca/news/2012/09/11/indian-brook-awash-in-flood-waters/

Berrang-Ford, L., and Noble, D. (2006). Climate Change and the Health of Canadians. Environ. Health Rev. 109–115.

Bruce, J., Burton, I., Martin, H., Mills, B., and Mortsch, L. (2000). Water Sector: Vulnerability and Adaptation to Climate Change. Final Report (The Government of Canada Climate Change Action Fund).

CBC News (2012). Heavy rains flood parts of central Nova Scotia. http://www.cbc.ca/1.1127913

Environment Canada (2009). Environment Canada - Water - Floods - Causes. http://www.ec.gc.ca/eau-water/default.asp?lang=En&n=E7EF8E56-1#snowmelt

Environment Canada (2010). Environment Canada - Weather and Meteorology - Public Alerting Criteria. http://www.ec.gc.ca/meteo-weather/default.asp?lang=En&n=D9553AB5-1#rainfall

Environment Canada (2011a). Canadian Climate Normals - Environment Canada. http://climate.weather.gc.ca/climate_normals/index_e.html

Environment Canada (2011b). Historical Climate Data - Environment Canada. http://climate.weather.gc.ca/climateData/dailydata_e.html?StationID=27141

Gilles, D., Young, N., Schroeder, H., Piotrowski, J., and Chang, Y.-J. (2012). Inundation Mapping Initiatives of the Iowa Flood Center: Statewide Coverage and Detailed Urban Flooding Analysis. Water *4*, 85–106.

Lewis, C.F.M., Taylor, R.B., Stea, R.R., Fader, G.B.J., Horne, R.J., MacNeil, S.G., and Moore, J.G. (1998). Earth Science and Engineering: Urban Development in the Metropolitan Halifax Region. In Urban Geology of Canadian Cities, P.F. Karrow, and O.L. White, eds. (Geological Association of Canada), pp. 409–444.

Madsen, T., and Willcox, N. (2012). When It Rains, It Pours Global Warming and the Increase in Extreme Precipitation from 1948 to 2011 (Environment America Research & Policy Center).

Mekis, E., and Hogg, W.D. (1999). Rehabilitation and analysis of Canadian daily precipitation time series. Atmosphere-Ocean *37*, 53–85.

Najjar, R.G., Walker, H.A., Anderson, P.J., Barron, E.J., Bord, R.J., Gibson, J.R., Kennedy, V.S., Knight, C.G., Megonigal, J.P., OConnor, R.E., et al. (2000). The potential impacts of climate change on the mid-Atlantic coastal region. Clim. Res. *14*, 219–233.

Natural Resources Canada (2010). Canada in a Changing Climate: Atlantic Canada. http://www.nrcan.gc.ca/earth-sciences/climate-change/community-adaptation/830

Neily, P.D., Quigley, E., Benjamin, L., Stewart, B., and Duke, T. (2003). Ecological Land Classification for Nova Scotia Volume 1 - Mapping Nova Scotia's Terrestrial Ecosystems (Nova Scotia Department of Natural Resources Renewable Resources Branch).

NS Dept. Env. (2009). Toward a Greener Future: Nova Scotia's Climate Change Action Plan (Nova Scotia Department of Environment). http://climatechange.gov.ns.ca/doc/ccap.pdf

Patro, S., Chatterjee, C., Mohanty, S., Singh, R., and Raghuwanshi, N.S. (2009). Flood inundation modeling using MIKE FLOOD and remote sensing data. J. Indian Soc. Remote Sens. *37*, 107–118.

Richards, W., and Daigle, R. (2011). Scenarios and guidance for adaptation to climate change and sea level rise-NS and PEI Municipalities.

Singh, D., Tsiang, M., Rajaratnam, B., and Diffenbaugh, N.S. (2013). Precipitation extremes over the continental United States in a transient, high-resolution, ensemble climate model experiment. J. Geophys. Res. Atmospheres *118*, 7063–7086.

Toreti, A., Naveau, P., Zampieri, M., Schindler, A., Scoccimarro, E., Xoplaki, E., Dijkstra, H.A., Gualdi, S., and Luterbacher, J. (2013). Projections of global changes in precipitation extremes from Coupled Model Intercomparison Project Phase 5 models. Geophys. Res. Lett. *40*, 4887–4892.

Weather Underground (2012). Weather History for Debert, NS. http://www.wunderground.com/

Webster, T., McGuigan, K., and MacDonald, C. (2011). Lidar processing and Flood Risk Mapping for Coastal Areas in the District of Lunenburg, Town and District of Yarmouth, Amherst, County Cumberland, Wolfville and Windsor.

Webster, T., Crowell, N., McGuigan, K., and Collins, K. (2012a). Integrated River and Coastal Hydrodynamic Flood Risk Mapping.

Webster, T., McGuigan, K., Crowell, N., and Collins, K. (2012b). River Flood Risk Study of the Nappan River Incorporating Climate Change.

Webster, T., Smith, T., and Collins, K. (2012c). Inventory of Physical Wastewater Infrastructure at Risk of Flooding to Climate Change induced Sea-level Incursions in the Minas Basin Area.

Whitfield, P.H., and Cannon, A.J. (2000). Recent Variations in Climate and Hydrology in Canada. Can. Water Resour. J. *25*, 19–65.

Zhang, X., Harvey, K.D., Hogg, W.D., and Yuzyk, T.R. (2001). Trends in Canadian streamflow. Water Resour. Res. *37*, 987–998.